Australian Government

Ansto

Nuclear-based science benefiting all Australians

Characterisation of the Neutron Field at the ANSTO Instrument Calibration Facility

Haider Meriaty

Quality, Safety, Environment, Radiation Protection, QSERP
Australian Nuclear Science & Technology Organisation, ANSTO

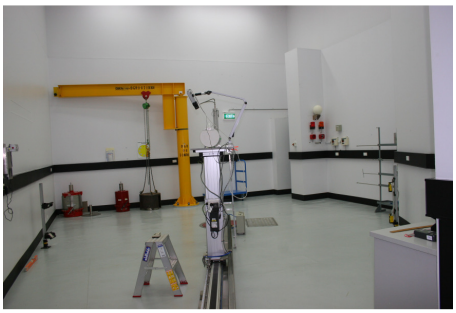

December 2009

Characterisation of the Neutron Field at the ANSTO Instrument Calibration Facility

Published by the Australian Nuclear Science and Technology Organisation.

ISBN	1 921268 123
ANSTO Report No.	ANSTO E-773
Front Cover	Neutron Calibration Hall at ANSTO Instrument Calibration Facility (ICF), December 2009
Photography	Haider Meriaty, ANSTO

Contact Details

ANSTO	Australian Nuclear Science and Technology Organisation New Illawarra Road, Lucas Heights, NSW, Australia
Postal Address	Locked Bag 2001 Kirrawee DC, NSW 2234, Australia
Telephone	+ 61 2 9717 3111
Facsimile	+ 61 2 9543 5097
Email	enquiries@ansto.gov.au
Internet	www.ansto.gov.au

Table of Contents

Abstract

ANSTO's Instrument Calibration Facility (ICF) provides calibration services to radiation monitors, used in radiation protection applications. The facility has a large calibration room that accommodates the neutron source rig and the monitor table, which is remotely controlled. The room also hosts the gamma calibration services.

Determination of the free field (direct) and scattered components of neutron field in a calibration room was essential to obtain an accurate response of the neutron monitor under testing. The free field fluence response and the fractional room return scatter, caused by the interaction of neutron fluence with the room structure, were determined. The fluence response was 1.210×10^{-4} μSv/h per n/m^2; and the neutron field has a fractional room scatter of 0.044 at 1 m and increases linearly versus square of distance.

The standard calibration methods, described by ISO-10647, IAEA-TR285, NCRP-112 and NPL-RS(EXT)5, were utilized in this characterisation and gave comparable results.

The shadow-shield (truncated cone) were found more suitable to describe the neutron field compared with the other methods e.g. the polynomial fitting, semi-empirical due to the fact of the size, shape of the ICF room and source/monitor positions. Nevertheless; all methods resulted in good response curves with correlation coefficients of fitting greater than 0.97.

The shadow shield consisted of two stacked conical sections. The first section was made from iron of 200mm height and the second section was a hollow and made from aluminium of 350mm height. The hollow section was then filled with neutron-moderating/absorbing materials i.e. water solution of LiBr 24% w/w. A performance test was conducted on the shield and gave a very satisfactory result e.g. the readings of fluence response to the free field neutron did follow the inverse square law with correlation >=0.999.

It is worth noticing that at the completion of this characterisation and report, the calibration results with the Physikalische-Technische Bundesanstalt (PTB) in Germany became available. As a result, the neutron characterisation at ICF calibration room did agree with the BTP calibration within five percent. Consequently, the neutron field in ICF rig calibration room is now traceable to BTP standard laboratory in Germany. Also, this agreement confirms the integrity of the current neutron source e.g. anisotropy stability, which should save substantial cost and efforts in replacing the source or sending it overseas for re-certification.

Keywords

neutron ambient dose equivalent, neutron monitor calibration, neutron field characterisation, monitor calibration with ^{241}Am/Be source, shadow shield calibration, neutron field characterisation at ANSTO-ICF.

INIS Descriptors

neutron monitors, BF_3 counters, long counters, radiation monitoring, scattering. calibration standards, interlaboratory comparisons.

1 Objectives

To determine the fractional room return scatter of a neutron field in the Instrument Calibration Facility (ICF) calibration room.

To determine the dose equivalent response of the ICF reference neutron monitor (Digipig2222).

2 Scope

This calibration applied to dose equivalent neutron monitors of type Digipig, Elinor, Studsvik or similar monitor using ^{241}Am/Be neutron source.

The front end of the monitor moderator shall face the neutron source. This arrangement is also called End-On or 0^{o} angle, in which the detector axis superimposes with the line of sight to the centre of the neutron source.

Throughout this report, the terms 'direct neutrons', 'cone' and 'distance' will refer to the free field neutrons, the shadow shield and effective distance (between source and monitor) respectively. They may be used interchangeably.

3 Methods

The shadow shield (a truncated-cone), the semi-empirical and the polynomial fitting methods were applied to determine the 'fractional room return scatter' and the monitor response. Details of these techniques are described in ISO standards[1,2,3] (8529, 8529-3, 10647), IAEA Technical Report Series[4] 285, NCRP Report[5] 112 and other relevant papers[6,7,8,9,10,11]. The results of these techniques were then compared.

The advantages and limitations of each technique are given in the ISO 10647 standard[3] and are summarised in the appendix of this report.

3.1 Shadow Technique, ISO10647

This method uses a truncated cone filled with neutron absorber to shield the monitor from the direct emission of a neutron source. The shield was placed halfway between the source and monitor. Nine measurements (M_S) were then taken between a range of 1 to 5 metres. At each position, the measurement was repeated five times; the measurement was carried out using the monitor's integral mode over a period of five minutes. However at 1 metre, the cone was placed closer to the source in order to provide a sufficient air gap at the monitor's front and optimise the deviation from the linear relation of air scatter required by the method. This limited source / monitor distance of 1 metre and the relatively long cone of 0.55m left only 0.45m air-total gap to be utilised.

Similar measurements (M_T) were repeated but without the shadow cone, which gave the total monitor reading of direct and scattered components of the neutrons. Therefore, the reading difference $\Delta M = M_T - M_S$ represents the net reading. This net should follow the inverse-square law[3] (ISL), providing it is corrected for all extraneous air scatter and geometry effects. The

distance (ℓ) in the ISL corresponds to the effective source-detector distance. The effective detector centre is marked on the monitor's moderator. ΔM is then given by the following equation:

(1) $$\Delta M \,.\, F_A(\ell) = k / \ell^2$$

Where:

- $F_A(\ell)$ is the corresponding air-attenuation factor (air-outscatter) as a function of distance.
- k is the source-detector Characteristic Constant i.e. monitor reading at unit distance, fully corrected for all scattering effects.

k value is determined by first order linear fitted function. Thus, a plot of $\Delta M.F_A(\ell)$ as a function of $(1/\ell^2)$ should illustrate a straight line with its slope equal to k value. The monitor response is then obtained from the relationship[3] between k, the fluence rate response (R_ϕ) and the neutron angular source strength (B_Ω).

(2) $$k = R_\phi \,.\, B_\Omega$$

The function in equation (1) should ideally have no intercept coefficient i.e. it passes through the coordinate's origin. Otherwise, any intercept value should be subtracted from the reading when this equation is applied in the client's routine calibration.

The fulfilment of measurement data with the ISL indicates a good integrity and functionality of a shadow shield.

3.2 Semi-Empirical Technique

This technique assumes that the fraction of the monitor reading, caused by the scattered neutrons, can be deduced from the reading's deviation from the inverse-squared law. The relationship between the monitor readings is considered as the sum of two components, which is brought about by the direct and scattered neutron fluences. The relationship represents the monitor's fluence response as a function of distance and is given in equation (3) below.

(3) $$M_T / [\phi \,.\, F_I(\ell) \,.\, (1 + A \,.\, \ell)] = R_\Phi \,(1 + S \,.\, \ell^2)$$

Where:

- A is the air scatter component. A=0.9% for ^{241}Am/Be source[3].
- S is the fractional room scatter contribution at unit test distance.
- ϕ is the neutron fluence rate.
- ℓ is the effective source detector distance.
- M_T is the total reading i.e. both direct and scattered neutrons.

A plot of left-hand side (LHS) of equation (3) versus ℓ^2 should yield a straight line. The intercept of the line with the LHS axis represents the R_ϕ value. The S value then corresponds to the line's slope divided by R_ϕ .

This technique[3] is usually suitable for a small room e.g. less than 2mx2mx2m in dimension.

3.3 Polynomial Fitting Technique

This technique utilises the equation[3] (4) below, which is derived from the semi-empirical equation (3) by expansion and ignoring the third order term that is relatively too small.

(4) $$M_T / [\phi \,.\, F_I(\ell)] = R_\Phi \,(1 + x \,.\, \ell + y \,.\, \ell^2)$$

Equation (4) is useful in obtaining or verifying the fluence rate response (R_ϕ). The x and y parameters should be regarded as fitting parameters i.e. no physical significance shall be ascribed to them namely room scatter, S. These parameters incorporate the correction for the total air scatter i.e. inscatter and outscatter.

Ten or more of data points are usually recommended[3] for a good fit.

3.4 NCRP112 Technique

NCRP Report[5] 112 recommends equation (5) below to obtain the fractional room return scatter factor (S).

(5) $$D.\ell^2 = D_o\,(1 + S.\ell^2)$$

Where:

D	is the monitor total reading, M_T.
S	is the line slope; it represents the scatter coefficient normalised at 1 metre.
D_o	is the deduced reading at 1 metre, from the source-neutrons exclusively.

In this approach, the total reading (M_T) of dose rate should be corrected for the corresponding air attenuation (F_A) and geometry (F_1) factors. The corrected values are then multiplied by the square of the corresponding distances. The results are then plotted as a function of distance squared (ℓ^2).

The IAEA Report[4] 285 illustrates a similar approach and the derivation of the equation.

3.5 Shadow Cone Assembly

A truncated cone was constructed similar to the one described in the NCRP Report[5] 112. However, the wax and Li_2CO_3 cone-section was replaced by a thin conical shell of aluminium filled with aqueous LiBr solution of 24%w/w concentration - the solution served as a moderator of fast neutrons as well as an absorber of the thermalised neutrons. This concentration was equivalent to the 10% w/w Li_2CO_3 suggested in the NCRP Report 112.

A total scattering comparison between paraffin wax and water was performed to assess their compatibility. Consequently, the scattering effects of the two moderators were found to be compatible and satisfactory. The details are listed in the relevant tables provided in the Tools and Instrumentation section.

A minimum mass of aluminium was used to construct the supporting table of the shadow cone. Also, minimum hydrogenous or thermal neutron absorbent materials were kept in the calibration room and at the same locations. These arrangements were intended to minimise the scatter effects and ensure the consistency of ambient conditions in the calibration room.

All measurements at a particular source-monitor distance were carried out over a fixed time period of five minutes and repeated five times.

Two cross-hair laser beams were utilised to align the source, cone and neutron monitor with an accuracy = < 1mm.

3.6 Data Manipulation and Fitting

Least Square Methods (LSM) were applied to fit data into polynomials function and determine their coefficients[12,13]. They included the Power and Orthogonal (Forsythe approach) Polynomials[14].

The power polynomials required intensive matrix treatments in order to obtain the polynomial coefficients. In addition, up to five measurement values could be fitted to avoid singularity of coefficient matrix e.g. ISO standard[3] recommends 10 data points for a good fit.

Alternatively, the Forsythe method accepts large number of fitting values and was later applied, compared with LSM results and adopted.

The general form of Forsythe orthogonal functions are:

(6) $$\mathbf{P_{j+1}(x) = (x - \alpha_{j+1})\, P_j(x) - \beta_j\, P_{j-1}(x)}$$

Where:

j is an integer ranges from -2 to n. It is the equivalent of the polynomials power.

α_{j+1} and β_j are parameters of real numbers and depend on the spacing of data points and orthogonal conditions.

Furthermore, α_{j+1} and β_j must fulfil the following relations over N measurement data, thereby satisfying the conditions that required for orthogonal polynomials.

(7) $$a_{j+1} = \frac{\sum_{k=1}^{N} x_k \cdot [P_j(x_k)]^2}{\sum_{k=1}^{N} [P_j(x_k)]^2}$$

(8) $$\beta_j = \frac{\sum_{k=1}^{N} x_k \cdot P_{j-1}(x_k) \cdot P_j(x_k)}{\sum_{k=1}^{N} [P_{j-1}(x_k)]^2}$$

The polynomial fitting technique in section (3.3) requires a second degree polynomial function, thus the value of n=1 was chosen. The corresponding set of Forsythe recursion functions was generated from the general function form and applied to the measurement data. The set had the following forms, with $\beta_0 = 0$.

$$P_{-1}(x) = 0$$
$$P_0(x) = 1$$
$$P_1(x) = (x - \alpha_1)\, P_0(x) - \beta_0\, P_{-1}(x)$$
$$P_2(x) = (x - \alpha_2)\, P_1(x) - \beta_1\, P_0(x)$$

The measurement data were applied to the following orthogonal polynomials and the appropriated quadratic fit function was obtained:

(9) $$\mathbf{y = b_0 \,.\, P_0(x) + b_1 \,.\, P_1(x) + b_2 \,.\, P_2(x)}$$

Where:

The polynomial coefficients b_i were obtained from the following relationship:

(10) $$b_i = \frac{\sum_{k=1}^{N} y_k \cdot P_i(x_k)}{\sum_{k=1}^{N} [P_i(x_k)]^2}$$

Where:

i	is 0,1 or 2.
k	is the index of N measurement data.
y_k and x_k	are the dependent and independent measurement datum respectively.

The above equations were programmed into an Excel Spreadsheet, Microsoft Office (97-2003) and used to fit and evaluate the experiment data.

3.7 Uncertainties

Type 'A' combined uncertainties[15,16,17] were applied to represent the statistical nature of measurement's errors.

Type 'B' uncertainties, given in ISO 10647 Standard[3], are also relevant to this work. They characterise the other uncertainties, which are caused by error sources that have a systematic effect on that particular measurement.

4 Materials

4.1 Lithium Bromine (LiBr)

24%w/w of high purity LiBr powder was dissolved in de-ionised water (conductivity = 0.02 Mega Ohm-cm). The solution provides a moderating and absorbing medium to neutrons. This concentration provided the equivalent 10%w/w concentration of Li_2CO_3, which suggested in NCRP Report[5] 112. The calculation of the adjustment factor for LiBr is detailed in the next section. This factor accounts for the molecular weight difference as well as the number of Li atoms per molecule.

4.1.1 Concentration-Adjustment Factor (CAF)

Volume of Aluminium-cone shell = 7.1 L or 7100 cm^3.
Water density = 1 g/cm^3.
Thus water weight = 1x7100 = 7100 g or 7.1kg.

Weight of 10% w/w Li_2CO_3 = 7.1x10/100 = 0.71 kg.
Molecular weight[18] of Li_2CO_3 = 74 g/mol.
Molecular weight[18] of LiBr = 87 g/mol.

Li is the absorber of thermal neutron. The ratio of Li abundance in the Li_2CO_3 and LiBr compounds is 2. On the other hand, their molecular weight ratio is 74/87= 0.85.
Therefore,
CAF = 2/0.85 = 2.4.

The required weight of LiBr, which gives the same absorption effect as per Li_2CO_3, is 0.71xCAF = 0.71x2.4 = 1.7 kg.
Therefore,
w/w% LiBr is 1.7/7.1x100 = 24%.

4.2 Preparation of LiBr Solution

LiBr salt dissolves in water exothermically, thus care must be taken during the solution preparation. As a guide, the following steps shall be applied for safe preparation and storage of the solution. ***Always wear the appropriate protective gear during this preparation.***

- Read the relevant chemical safety datasheets thoroughly e.g. MSDS.
- Place the solving container in a suitable heat-sink e.g. sink-basin and running water. Fill the container to 50 percent of total solution volume.
- Add a small portion of the LiBr granulates (e.g. 10 percent of the total mass of the salt at one time) into the container.
- Monitor the solution temperature and ensure that it stays below 60 ^oC.
- When all the salt is added, top up the solution to the required cone volume.
- Transfer the final solution, as soon as practical, into the cone-shell and secure its cap.

If the cone-shell is not internally coated with inert film e.g. wax or polyurethane, the solution will react slowly with the shell wall and generate gas that will deform the cone shape as well as cause the fracture/explosion of the shell. **Therefore, the filled cone should not be retained for more than one day**. Alternatively, you **MUST** empty it and store it in a plastic drum for future re-usage.

The LiBr solution must not be exposed to room air temperature for an extended time e.g. > 30 minutes. If it does it will absorb the ambient CO2 and form a Li_2CO_3 compound, which precipitates and consequently affects the distribution uniformity and initial concentration of the solution.
If the filled cone is not required for extended period of time e.g. months, transfer the solution into an appropriate plastic container and secure its cap (i.e. air tight). Place the container into a suitable drum (spill barrier) and store them in a safe and approved location.

The following specifications of Lithium Bromide (LiBr) granulates were applied to prepare the cone-solution (see the table below).

Table 1: Specifications summary of the LiBr compound used in the solution preparation of a thermal neutron absorber.

Formula	*LiBr*
Formula Weight	*86.85*
Purity	*>=99%*
Density	*3.464*
Brand	*Fluca, Cat.:62463*
CAS code	*7550-35-8*
Lot	*S40883 32907B16*

Supplier	*Sigma-Aldrich, Sydney, Australia*
Product of	*Germany*

4.3 Trays and Cone Shell

A hollow truncated cone section (shell) and two trays were fabricated from aluminium sheets. The sheet had the following industry identification: 1100 Alloy and O Temper as per ASME SB209, which was supplied by Calm Aluminium PTY LTD.

The trays fitted onto the top of the stand and formed a supporting table. The shell mounted in an aluminium cradle, made of the same sheet grade, and the combination was then positioned on the supporting table during the measurements.

The maximum impurities (listed in Table 2), given in the material certificate as a weight percentage, corresponded to a total impurity percentage of 0.63 percent. Rows six and nine in the table give the weights of each individual impurity for the cone (W_{shell}) and trays (W_{trays}) respectively.

The total weight of the truncated-cone shell, including its cap was 628.8g.

The trays' average size= 40x30cm and the total thickness was 2.4mm. Tray one and tray two weigh 1080±20g and 1060±20g respectively (the total weight of both trays = 2140±20g). One tray can fit into the other.

The macroscopic cross sections (whole target) of scatter (Σ_s) and absorption (Σ_a) of fabricated aluminium materials and their impurities for the cone-shell and trays are listed in Table 2.

It was evident that the scatter and absorption effects caused by the impurities were relatively much less than aluminium; and overall insignificant for the shell or trays.

Table 2: w/w% of impurities in aluminium sheets used in the fabrication of the cone shell and trays. The macroscopic cross sections of these impurities are much less than the aluminium.

	Al	Si	Fe	Cu	Mn	Mg	Cr	Ni	Zn	Ti
A (g)	26.98	28.09	55.85	63.54	24.31	54.94	52	58.71	65.37	47.9
w/w%	99.37	0.09	0.4	0.07	0.03	0.007	0.001	0.006	0.005	0.02
σ_s (b)	1.5	2.17	11.62	8.03	2.15	3.71	3.49	18.5	4.13	4.35
σ_a (b)	0.23	0.17	2.56	3.78	13.3	0.06	3.05	4.49	1.11	6.09
W_{shell} (g)	624.84	0.57	2.52	0.44	0.19	0.04	0.01	0.04	0.03	0.13
Σs (cm-1)	**2.09E+01**	**2.63E-02**	**3.15E-01**	**3.35E-02**	**1.00E-02**	**1.79E-03**	**2.54E-04**	**7.16E-03**	**1.20E-03**	**6.88E-03**
Σa (cm-1)	**3.21E+00**	**2.06E-03**	**6.94E-02**	**1.58E-02**	**6.21E-02**	**2.89E-05**	**2.22E-04**	**1.74E-03**	**3.21E-04**	**9.63E-03**
W_{trays} (g)	2126.54	1.93	8.56	1.50	0.64	0.15	0.02	0.13	0.11	0.43
Σs (cm-1)	**7.12E+01**	**8.96E-02**	**1.07E+00**	**1.14E-01**	**3.42E-02**	**6.09E-03**	**8.65E-04**	**2.44E-02**	**4.07E-03**	**2.34E-02**

A : Atomic mass.
w/w% : weight to weight percentage of impurity.
σ_s : microscopic scatter cross section[19] in barn (b) = 10^{-24} cm^2.
σ_a : microscopic absorption cross section[19] in barn (b) = 10^{-24} cm^2.
W_{shell} : total weight of impurities in the shell.
W_{trays} : total weight of impurities in the trays.
Σ_s : macroscopic cross sections of scatter (whole target).
Σ_a : macroscopic cross sections of absorption (whole target).

4.4 Support Stand

An aluminium stand was fabricated and its top was designed and sized to fit the trays onto it so as to form a supporting table. The assembly of cone and cradle was placed on the table top during measurements (see Figure 2).

Hollow aluminium rods of a total mass = 3560g were used to fabricate the stand. The industry specifications of the rods were as follows: Alloy: 60601 and Temper: T6, which was supplied by Calm Aluminium, CA in the USA.

The following maximum impurities were listed in the material certificate as weight percentage. This equated to 95.85 percent aluminium, hence the net mass of aluminium in the rods was [(3560x95.9)/100] = 3412.26g.

The weight of the stand was 3560±20g. Thus, the weight difference accounted for the auxiliary masses such as welding and screws at the stand's legs. These additional masses were considered insignificant, thus were not included in the cross section evaluation.

The macroscopic cross sections of scatter and absorption (whole stand) of aluminium and their impurities are listed in Table 3.

It was evidence that the scatter and absorption effects caused by the impurities were relatively much less than aluminium.

Table 3: w/w% of impurities in aluminium rods type which are used in fabrication of the support stand. The macroscopic cross sections of these impurities are much less than the aluminium.

	Al	Si	Fe	Cu	Mn	Mg	Cr	Zn	Ti	Others
A (g)	26.98	28.09	55.85	63.54	24.31	54.94	52	65.37	47.9	
w/w%	95.85	0.8	0.7	0.4	0.15	1.2	0.35	0.25	0.15	0.15
σ_s (b)	1.5	2.17	11.62	8.03	2.15	3.71	3.49	4.13	4.35	
σ_a (b)	0.23	0.17	2.56	3.78	13.3	0.06	3.05	1.11	6.09	
W_{frame} (g)	3412.26	28.48	24.92	14.24	5.34	42.72	12.46	8.90	5.34	5.34
Σs (cm-1)	**1.14E+02**	**1.32E+00**	**3.12E+00**	**1.08E+00**	**2.84E-01**	**1.74E+00**	**5.03E-01**	**3.38E-01**	**2.92E-01**	
Σa (cm-1)	**1.75E+01**	**1.04E-01**	**6.88E-01**	**5.10E-01**	**1.76E+00**	**2.81E-02**	**4.40E-01**	**9.10E-02**	**4.09E-01**	

A (g) : Atomic mass.
w/w% : weight to weight percentage of impurity.
σ_s : microscopic scatter cross section[19] in *barn* (b) = 10^{-24} cm^2.
σ_a : microscopic absorption cross section[19] in *barn* (b) = 10^{-24} cm^2.
W_{frame} : total weight of impurities in the aluminium frame.
Σ_s : Macroscopic cross section of whole target.
Σ_a : Macroscopic cross section of whole target.

4.5 Iron Section of Shadow Cone

The top part of the shadow cone was made of a solid iron section[3,5]. This section was fabricated from iron ingot of grade Flocast MF2. The maximum chemical compositions, given by the material Analysis Certificate, are listed as weight percentage in Table 4, row three. The volume of this section was 568cm^3 and would weigh 4.47kg (using Fe density value[18] = 7.86g/cm^3). The corresponding weights of the impurities in the section are listed in row six.

The macroscopic cross sections of scatter and absorption (whole section) of iron cone and their impurities are listed in Table 4.

It was evident that the scatter and absorption effects caused by the impurities were relatively much less than iron.

Table 4: w/w% of impurities in iron ingot type which were used in the solid section fabrication of the shadow cone. The macroscopic cross sections of these impurities were much less than the iron (Fe).

	Fe	P	Si	Mn	C	Ti
A (g)	55.85	30.97	28.09	24.31	1201	47.9
w/w%	92.47	0.03	2.9	0.6	3.8	0.2
σ_s (b)	11.62	3.31	2.17	2.15	5.55	4.35
σ_a (b)	2.56	0.17	0.17	13.3	0.004	6.09
W_{cone} (g)	4133.41	1.34	129.63	26.82	169.86	8.94
Σs (cm-1)	**5.18E+02**	**8.63E-02**	**6.03E+00**	**1.43E+00**	**4.73E-01**	**4.89E-01**
Σa (cm-1)	**1.14E+02**	**4.43E-03**	**4.72E-01**	**8.83E+00**	**3.41E-04**	**6.84E-01**

A (g) : Atomic mass.
w/w% : weight to weight percentage of impurity.
σ_s : microscopic scatter cross section[19] in *barn* (b) = 10^{-24} cm^2.
σ_a : microscopic absorption cross section[19] in *barn* (b) = 10^{-24} cm^2.
W_{cone} : total weight of impurities in the conical iron section.
Σ_s : Macroscopic cross section of whole target.
Σ_a : Macroscopic cross section of whole target.

4.6 Neutron Source

The calibration room rig at the Instrument Calibration Facility (ICF) houses one neutron source and other gamma sources. It also has a spare position for an extra source. The specifications[20,21] of the neutron source used in this evaluation are listed in the table below. The decay factor was referenced on the measurement date of 8 December 2009.

Table 5: Specifications of the neutron source in the ICF Rig calibration room. . Measurement dates were 4, 8 and 9 December 2009. The decay factor was referenced on the measurement date 8 December 2009.

Emission @ measurement date (s^{-1})	Activity @ measurement date (Bq)	Decay Correction Factor	Reference Emission[25] (s^{-1})	Reference Activity (Bq)	Half Life (day)
2.081E+07	3.32E+11	0.956	2.176E+07	3.47E+11	*157850 (432.5 yr)*
Measurement Date	**Elapsed Days**	**Source Serial Number**	**Reference Date**	**Capsule Type[26]**	***Active section (mm)***
8/12/2009	*10165 (27.8yr)*	*4232 NE*	25/02/1982	*X.14*	*20Hx27.6Dia*

5 Tools and Instrumentation

5.1 Shadow Shield Assembly

This assembly consisted of two conical sections and an aluminium cradle. The conical sections were horizontally fitted onto the cradle and formed one truncated cone. The cradle was equipped with vertical plates to support each conical section as well as aligning their axes.

The slant of the cone's side was at an angle of 10.3^{o} degrees to its central axis. The following linear equation was derived to describe the cone-slanted side, thus to match the required physical size for shadow technique[5] setup (see Figure 1). This equation was used later to calculate the volume (v) of the conical sections.

(11) $$\mathbf{y = 0.1818\ x + 1}$$

Where:

'y' represents the cone's radius at height 'x'.

The cone volume was calculated using the three dimensional integration method[13] of revolving function. Hence, the conical volume was generated when the linear function 'y' in equation (12) revolved around the coordinate axis 'x' and integrated between the desired height limits. The intercept value with the 'oy' axis corresponded to the radius of the smaller cross section of truncated cone (i.e. radius = 1cm). Therefore, the conical volume (v) was obtained by applying the following equation.

(12) $$\mathbf{v = \pi \int (0.1818\ x + 1)\ .\ dx}$$

This equation was programmed into Mathematica[22] software package (version 5) and integrated to obtain the volumes and masses of conical sections.

Figure 1: Diagram of shadow cone and its sections. The narrow side faced the neutron source and the wider one faced the monitor.

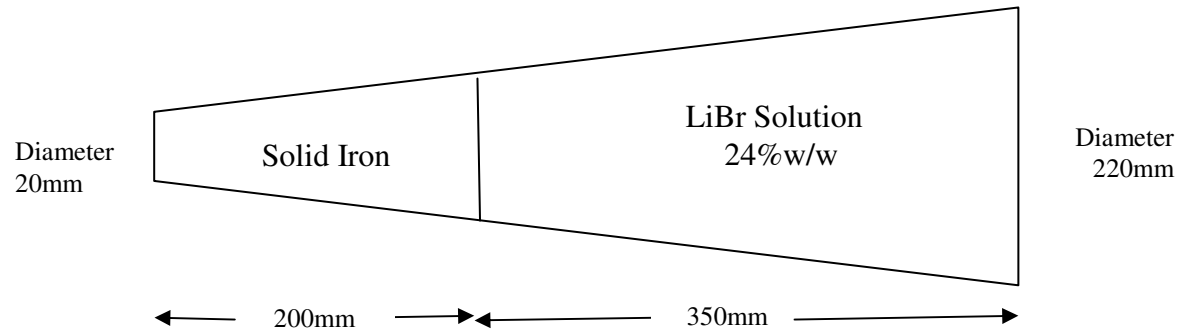

The features and specifications of the shadow cone assembly (cone block and cradle) were listed in Table 6. The cone shell was filled with the LiBr solution.

Table 6: Features of shadow cone assembly. The assembly consisted of two conical sections and a supporting cradle. D1 and D2 are the diameters of the truncated cones.

		Truncated-Cone		Shell's Filling	Cradle
		Section-1	***Section-2***		
Solidity		Solid	Shell	Solution	Solid
Diameters, (mm)	**D1**	20	92.72	92.72	-
	D2	92.72	220	220	
Height, x (mm)		200	350	350	
Volume (cm^3)		568.2	7090.8	7090.8	-
Length (mm)		-	-	-	350
Width (mm)		-	-	-	220
w/w% Concentration		~100 Iron, casted	~100 Al alloy	24 LiBr/H2O	~100 Al alloy
Shape		Truncated Cone	Truncated Cone	Truncated Cone	Rectangle with Vertical Pillars
Composition		Fe	Al	LiBr in H2O	Al
Weight (kg)		4.47	0.629	8.288	0.55
Wall Thickness (mm)		-	1.2	-	1.2

5.2 Materials' Effects on Neutron Scatters and Absorptions

Neutron moderating and absorbing properties of the shadow cone were evaluated and summarised in Table 7. The overall percentages of the cross sections of involved materials represented the total atomic constituents and listed in column "sum%". The σ_s and σ_a represent the microscopic cross sections of scatter and absorption of neutrons respectively.

5.2.1 Absorption of Thermal Neutrons

Table 7 illustrates the comparison results between LiBr and Li_2CO_3 compounds of the absorption and scattering properties of thermal neutrons. Columns five and six give the ratio of compound cross sections (i.e. cross-sectional sum of atomic constituents of the molecules). Two molecules of LiBr were used in the calculations in order to account for the extra Li atom in the Li_2CO_3 compound.

The results indicated that LiBr has advantage over the Li_2CO_3 compound e.g. 9.7 percent higher absorption and 31 percent less scatter cross sections.

In addition, water (as a solvent) possesses a short Diffusion Length[23] (L = a few centimetres; details are given in the next section). Thus, the majority of the scattered neutrons take place within the solution and are eventually absorbed with minimal additional scatter outside the cone. Furthermore, C and O atoms would have insignificant effects due to their very large L values.

Table 7: Comparison results of the neutron cross sections of two compounds used as absorbers of thermal neutron for shadow cone. The LiBr compound has an advantage over Li_2CO_3 in terms of less scatter and more absorption of neutrons.

Neutron Cross Section of Li_2CO_3 (b)				Sum%		Neutron Cross Section of 2LiBr (b)			
Element	Abandance Fraction	σ_s	σ_a	σ_s	σ_a	Element	Abandance fraction	σ_s	σ_a
Li-6	0.0759	0.97	940			Li-6	0.0759	0.97	940
Li-7	0.9241	1.4	0.045			Li-7	0.9241	1.4	0.045
C	1	5.56	0.004			Br-79	0.5069	5.96	11
nil	0	0	0			Br-81	0.4931	5.84	2.7
O	1	4.23	0.0001						
Li_2CO_3 (b)		**20.98**	**142.78**	**0.69**	**109.67**	**2LiBr (b)**		**14.54**	**156.59**

(b): *barn* = 10^{-24} cm^2.

5.2.2 Moderation of Fast Neutrons

The moderating properties of paraffin wax and water were evaluated and compared. The results demonstrated comparable Diffusion Lengths[23] (L) e.g. in order of a few centimetres for hydrogen. L value incorporates the competing effects of the two types of cross sections, e.g. absorption and scattering (see Table 8). The terminologies and their meanings, given in the table, are explained in the following paragraphs.

Table 8: Comparison results of thermalised neutron properties of two compounds that were considered in shadow shield construction.

		Paraffin Wax		Water	
Molecular Formula[24]		$C_{25}H_{52}$		H_2O	
Hydrogen Ratio		2.08		2	
Molecular Weight (g/mol)		352		18	
Molecular Density (mol/cm^3)		1.59E+21		3.34E+22	
Atomic Density ($Atoms/cm^3$)		**H**	**C**	**H**	**O**
		8.27E22	3.98E+22	6.69E+22	3.34E+22
Microscopic Cross Sections (b)	σ_a	0.33	0.004	0.33	0.0001
	σ_s	82.03	5.56	82.03	4.23
Macroscopic Cross Sections (cm^{-1})	Σ_a	2.73E-02	1.59E-04	2.21E-02	3.34E-06
	Σ_s	6.78E+00	2.21E-01	5.49E+00	1.41E-01
Mean Free Path (cm)	λ_a	3.66E+01	6.29E+03	4.53E+01	2.99E+05
	λ_s	1.47E-01	4.52E+00	1.82E-01	7.07E+00
	λ_{tr}	0.69	2931.81	0.85	8144.25
Average Cosine of Deflected Angle (Lab-System)	μ	0.786	0.998	0.786	0.999
Diffusion Length (cm)	**L**	**2.90**	2479.3	**3.59**	28490.5

(b): *barn* = 10^{-24} cm^2.

The molecular density represents the actual number of molecules per cubic centimetre of a compound.
The atomic density is equal to the molecular density times the number of atoms. It was then applied to calculate the corresponding macroscopic cross sections of an intended compound.
The Mean Free Path[23] ($\lambda_{a/s}$) of absorption or scattering represents the total path that a neutron traces before absorbed or scattered by the medium. It is given as $\lambda_{a/s} = 1/N.\sigma_{a/s}$ where N is the number of nuclei per cubic centimetre in a medium.

The Transport Mean Free Path is a function of λ_s and the Scattering Angle (θ). It is given as $\lambda_{tr} = \lambda_s/[1-\cos(\theta)]$.

The Diffusion Length constant[23] (L) represents the average distance (line of sight) that a neutron moves from its initial plane before absorption. It concurrently combines λ_a and λ_{tr} effects and is defined by the following relationship: $L = [(\lambda_a .\lambda_t)/3]^{1/2}$.

Consequently, the Paraffin or water media exhibited comparable effects on the neutron slowing down range as illustrated by the calculated L values of hydrogen.

5.3 Neutron Monitors

The ICF reference neutron monitor was used throughout the characterisation measurements of the rig calibration room. The monitor had an ANSTO tag indicating an *in situ* check of reading consistency, valid up to 10 March 2010. It was manufactured by Wedholm Medical in Sweden (www.wedholmmedical.se). However, the monitor had no documentation of traceability to standard calibration authority. A traceable calibration was then sought to be initiated once this characterization completed, thus avoiding any delay to the work. Furthermore, the calibration factor provided by the authority will then be applied to the final characterisation outcomes prior to commissioning of the calibration room for routine neutron services to clients.
The monitor calibration typically takes four to six months by an external recognisable standard laboratory.

The manual[25] of the ICF monitor includes a Test Certificate no Kp-06067 dated 17 December 2007. The monitor's certificate reported a neutron sensitivity of 0.40 cps/microSv/h and a good linearity.

The Digipig monitor (2222A) employed a BF3 detector, polyethylene moderator, borated plastic absorber and digital display. The monitor's energy response was in close agreement with an ICRP74 neutron sensitivity response curve.

The monitor has several measurement modes such as dose rate and accumulated dose (updated at 100 seconds interval). A summary of the ICF monitor's specifications are listed in the table below.

Table 9: A summary of features and specifications of the reference neutron monitor used at ICF.

Description	**Unit**	***Value***
Brand	-	Digipig
Model		2222A
Serial number	-	2222.0128
Energy response	MeV	0.025-17
Angular response between 0^o to ± 75^o, reference to detector's axis at the middle of moderator.	Deg	± 1 to 1.13
Angular response between 75^o to ± 90^o, reference to detector's axis at the middle of moderator.	Deg	1.0
Neutron sensitivity	cps/(μSv/h)	0.4
Gamma sensitivity per 2 Gy/h	μSv/h	< 5
Dose rate range (digital display)	mSv/h	0.001 – 999.8
Dose range	-	0.01μSv to 999.8mSv
Distance of effective centre of detector from the moderator's front end to the marker (black grooved around the moderator).	mm	124
Moderator diameter	mm	215
Moderator length	mm	230
Voltage plateau of detector	V_{DC}	2300 - 2700
Plateau slope	Deg.	~ 2% per 100V
Warning of low voltage of power supply	-	yes
Traceability to standard authority	-	pending

5.4 Timer

A digital timer was used to time the integrated monitor dose over a five minute period, with an accuracy of one second; the monitor ran in "Integral Dose" mode.

The timer model was 870A and supplied by a local Dick Smith Electronics shop (Sydney, Australia).

5.5 Correction Factors & Parameters

The air attenuation (F_A) and geometry (F_1) correction factors are required in the equations of all three techniques. Their relevant parameters and values, as a function of the effective distance (ℓ) between neutron source and monitor, are listed in Table 10.

The value of F_A as a function of distance and neutron energy was calculated from equation (13) and Annex E data in reference 3. Here Σ represents the macroscopic cross section of air at a temperature, pressure and humidity of $21C^o$, 100.4kPa and 50 percent respectively.

The ICF calibration room is fitted with a temperature controlled system. Fulfilment of the above temperature and humidity conditions was assumed, although the room did not have a display or gauges to verify the conditions' values.

(13) $$\mathbf{F_A(\ell,E) = \exp(\ell.\Sigma(E))}$$

The value of F_1 was calculated from the following equation[3], in which 'r' represents the radius of sphere or cylinder.

(14) $$F_1(\ell) = 1 + \delta \,.\, (r/2 \,.\, \ell)^2$$

The values of Σ and δ, used in the equations of the correction factors, were taken from the ISO 10647 standard[3] for ^{241}Am/Be source. Also, the value of total air scatter (A) used in the semi-empirical equation was taken from the same reference.

Values of F_A and F_l related to the monitor and calibration room of ICF are listed in Table 10.

Table 10: A list of air attenuation (F_A), geometry (F_1) and correction factors as a function of the effective distance (ℓ) between neutron sources and the monitor. Also, parameters used in the calculations are also listed:

Effective Distance, ℓ (m)	ℓ^2 (m^2)	F1(ℓ)	δ (effectiveness parameter)	Air-Scatter parameter, A	Air-Attenuation Correction, F_A(l)	Σ (m^{-1})
0.12	0.0144	1.1003			1.0011	
0.25	0.0625	1.0231			1.0022	
0.5	0.25	1.0058			1.0045	
1	**1**	**1.0014**	**0.5**	**0.009**	**1.0089**	**0.0089**
1.5	2.25	1.0006			1.0134	
2	4	1.0004			1.0180	
2.5	6.25	1.0002			1.0225	
3	9	1.0002			1.0271	
3.5	12.25	1.0001			1.0316	
4	16	1.0001			1.0362	
4.5	20.25	1.0001			1.0409	
5	25	1.0001			1.0455	

6 Calibration Room

The ICF calibration room has a solid concrete floor and is surrounded by double walls with a total thickness of about 600mm. The walls are built from solid concrete blocks. The internal faces of the walls are lined with gypsum panels of 20mm thickness. The height of these panels is about 75 percent of the wall's height.

The dimensions of the room are shown on the engineering plan (see Figure 2). The guide tube of the source is positioned at the centre of the room's widest section. The radius between the source-guide to the closest wall is 3.4 metres.

The room's roof is made of metal alloy (e.g. collar-bond) and positioned at a height = 9300mm. A standard "false" ceiling is also installed in the room at a height = 6000mm.

The rig system is equipped with an aluminium calibration table of adjustable height. The table movement along the rail-guide is computer-driven (from the control room) and has a range of 200mm to 5000mm from the source. The accuracy of table displacement is less than 2mm.

The rail is bolted to the room's floor and oriented diagonally to minimise the wall's scatter.

A vacuum system forces the neutron source to travel upward and vertically hold at a height = 1640mm.

Figure 2: Photos showing the interior and instrument arrangements of the ICF calibration room taken at different perspective angles. They include the arrangements with and without the shadow shield. The two-step ladder was removed to the side of the wall (left) during the measurements. The figure includes the floor plan of the room, showing the location of the sources rig and the rail of the calibration table.

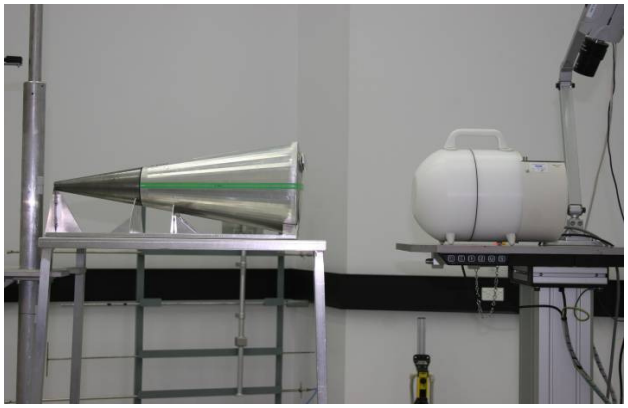

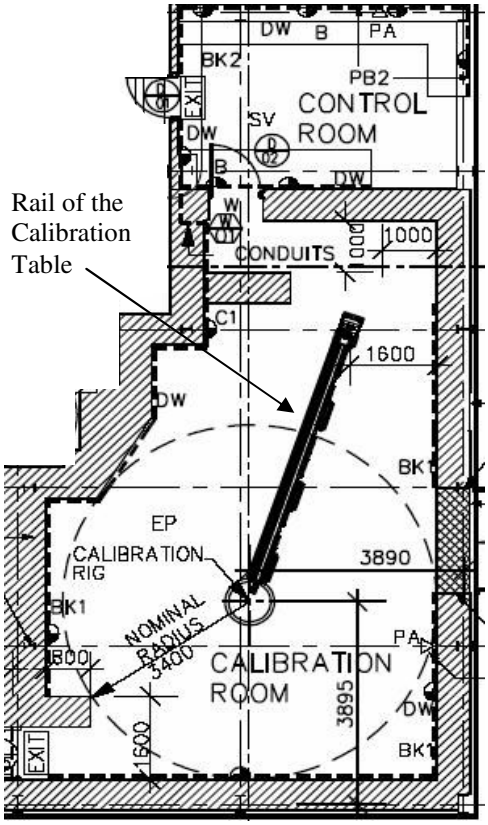

7 Setup and Acquisitions

7.1 Shadow Shield Assembly

The support table was positioned half way between the neutron source and rail-calibration stand. The shadow shield assembly was then placed on the support table, where the narrow cone's end faced the source (Fig 2).

The monitor was placed on the rail-stand and its effective centre mark aligned with the rail's distance marker. The stand was positioned at the desired distance from the control room. The monitor's front face (the moderator's base) was pointed toward the source (0^o angle between the line of sight and the moderator's axis).

The combination of the mid-source was sagittally and laterally aligned with the axes of shadow shield as well as the monitor's moderator, using the cross hair of two laser units and reference markers on the walls of the ICF rig-room. The accuracy of the alignment was < 1mm.

The monitor reading was viewed via the CCT camera / monitor system from the control room and recorded by the operator.

7.2 Neutron Monitor

The 'Integral' mode of monitor reading was applied over a period of five minutes. A digital timer was used to keep track of the measurement period.

The operator used a two-step aluminium ladder to reach the monitor display and the CCTV camera. The operator activated the timer and monitor's acquisition concurrently, descended to the room floor and moved the ladder next to the tool bench and then left the room quickly.

7.3 Acquisitions

Measurements were taken at nine positions, covering a range from 1 metre to 5 metres at an interval of 0.5m. At each interval, five accumulative readings were recorded at five minute intervals. The net monitor reading at each time segment was then calculated by taking the difference between the current and last reading. The source transit time was avoided by taking an extra reading initially.

Every session of measurement was proceeded by a background measurement of the ICF room over a period of 15 minutes (at least) and found to be zero. Also, the battery status was checked and replaced if required. The solution level in the cone shell was also checked prior to and after each measurements session. No additional filling was required throughout the measurements.

8 Results and Analysis

8.1 Free-Field Fluence and Dose Rate

The reference neutron fluence, given in the NPL Calibration Certificate[20], was corrected for decay to the measurement date (8 December 2009) and then applied to calculate the expected

free field fluence and rates as a function of distance. The fluences were also corrected for the corresponding air attenuation.

The neutron fluences listed in column two of Table 11 were obtained by dividing the emission at the measurement date (Table 5) by the corresponding solid angle.

The conversion factor[2] of fluence to ambient dose $^{*}H(10) = 3.91E\text{-}14$ (Sv/m^2) was applied to obtain the ambient dose equivalents of free field neutron at the ICF rig calibration room.

Table 11: List of the fluences and dose rates of the neutron source (4232 NE) at the ICF rig calibration room. The free field values of neutron fluences in column two were multiplied by *H(10) to convert them to the corresponding dose rates and given in column six. The values in column four represent the attenuated dose rates (column three values divided the correspondence values of the air attenuation correction factor $F_A(\ell)$ given in column five).

Distance, ℓ (m)	Neutron Fluence, [free field] (n/m^2)	Source Dose Rate [free field] (μSv /h)	Air-Attenuated Source Dose Rate (μSv /h)	$F_A(\ell)$	Source Dose Rate [free field] (Sv/s)	Source Dose Rate, [free field] (Sv/h)
0.12	1.151E+08	1.620E+04	1.618E+04	1.0011	4.499E-06	1.620E-02
0.25	2.651E+07	3.732E+03	3.723E+03	1.0022	1.037E-06	3.732E-03
0.5	6.627E+06	9.329E+02	9.287E+02	1.0045	2.591E-07	9.330E-04
1	**1.657E+06**	**2.332E+02**	**2.312E+02**	**1.0089**	**6.478E-08**	**2.332E-04**
1.5	7.364E+05	1.037E+02	1.023E+02	1.0134	2.879E-08	1.037E-04
2	4.142E+05	5.831E+01	5.728E+01	1.0180	1.620E-08	5.831E-05
2.5	2.651E+05	3.732E+01	3.649E+01	1.0225	1.037E-08	3.732E-05
3	1.841E+05	2.591E+01	2.523E+01	1.0271	7.198E-09	2.592E-05
3.5	1.353E+05	1.904E+01	1.845E+01	1.0316	5.288E-09	1.904E-05
4	1.036E+05	1.458E+01	1.407E+01	1.0362	4.049E-09	1.458E-05
4.5	8.182E+04	1.152E+01	1.106E+01	1.0409	3.199E-09	1.152E-05
5	6.627E+04	9.329E+00	8.923E+00	1.0455	2.591E-09	9.330E-06

The free field of neutron fluences in column two of Table 11 were multiplied by *H(10); hence converted to the corresponding dose rates, which are given in column six. The dose rates per hour per fluence in column seven were obtained by multiplying column six values by 3600 factor (i.e. seconds per hour) to provide an alternative common unit of dose rate (μSv /h).

The values in column four represent the air attenuated dose rates. They were obtained from the free field values of dose rate (column three) divided by the correspondence values of the air attenuation correction factor $F_A(\ell)$ given in column five.

The distance (ℓ) represents the effective distance between the neutron source and the effective centre of neutron monitor.

A conversion factor of ICF free field fluence to an hourly dose rate at 1 metre was obtained by taking the ratio of values in third and second columns as follows.

$$\mathbf{h_{\Phi}(ICF) = 2.332e2 / 1.657e6 = 1.407e\text{-}4\ \mu Sv\ /h\ per\ n/m^2}$$

Further, this factor was almost constant within a range of 0.25 to 3.5 metres but diverts slightly beyond it.

8.2 Dose Rate Measurements

The monitor readings at the desired distances, with and without the shadow cone, are listed in Table 12. The distance 'ℓ' represents the direct distance between the source-central axis and the effective-centre of the monitor. The effective centre was marked by a black groove around the moderator. The effective centre was 124mm away from the front face of the moderator.

The total and shadow measurements were obtained in two separate sessions. The Total Dose Rate, M_T represents the reading of the free field and scattered components of the incident neutrons on the monitor.

The Shadow Dose Rate, M_s represents the scatter reading while the shadow shield was positioned at the middle distance between the source and monitor blocking the direct neutrons.

Measurements at 1 metre were performed with the shadow cone placed closer to the source rather than at an equidistance, in contrast with the rest of measurements. However, this arrangement was necessary to allow a sufficient air gap between the cone face and the monitor, so optimising the linear relation[3,4,11] between air inscatter and net scatters (i.e. inscatter minus outscatter). The recommended ratio[3,4] of gap to cone length is of order of one or more in order to obtain a linear net scatter with uncertainty < three percent.

The distance between the cone's small face and source was set at 50mm. This arrangement provided a gap of 400mm, which corresponded to 73 percent of the recommended ratio[3,5]. Details of the calculation are as follows.

Source to monitor distance	= 1000mm
Shadow cone length	= 550mm
Source to cone's front face (small)	= 50mm
Monitor to cone's rear face (large)	= 1000 - (550 + 50) = 400mm
Ratio	= 400 / 550 = 0.73

Table 12: List of the initial reading values by the ICF monitor with and without the shadow shield. The Total Dose Rate corresponded to the direct and scattered neutrons detected by the monitor. The shadow Dose Rate corresponds to the scattered neutrons only.

Distance, ℓ (mm)	Total Dose Rate, M_T (μSv/5min)	Shadow Dose Rate, M_s (μSv/5min)
1000	**19.114**	**2.6**
1000	**19.11**	**2.618**
1000	**19.48**	**2.643**
1000	**19.11**	**2.61**
1000	**19.25**	**2.63**
1500	9.399	2.189
1500	9.244	2.177
1500	9.37	2.19
1500	9.41	2.204
1500	9.09	2.2
2000	**5.708**	**1.815**
2000	**5.649**	**1.821**
2000	**5.74**	**1.784**

2000	**5.7**	**1.814**
2000	**5.78**	**1.764**
2500	4.041	1.604
2500	4.163	1.525
2500	4.086	1.585
2500	4.16	1.614
2500	4.07	1.575
3000	**3.109**	**1.417**
3000	**3.226**	**1.415**
3000	**3.153**	**1.437**
3000	**3.197**	**1.424**
3000	**3.16**	**1.417**
3500	2.532	1.204
3500	2.593	1.253
3500	2.572	1.248
3500	2.582	1.277
3500	2.52	1.239
4000	**2.077**	**1.172**
4000	**2.077**	**1.13**
4000	**2.118**	**1.105**
4000	**2.168**	**1.187**
4000	**2.022**	**1.145**
4500	1.749	1.043
4500	1.765	1.051
4500	1.783	0.969
4500	1.785	1.018
4500	1.848	1.035
5000	**1.531**	**0.882**
5000	**1.568**	**0.899**
5000	**1.567**	**0.934**
5000	**1.528**	**0.951**
5000	**1.535**	**0.965**

The readings of initial measurements were averaged at each distance and listed in Table 13 with their associated statistical sample standard deviations. These values were then utilised to obtain the relevant characterisation parameters of the neutron field and rig-calibration room.

Table 13: List of the average dose rate readings of total and shadow configurations obtained by the ICF neutron monitor. Their associated sample standard deviations (SD) were also listed.

Distance, ℓ (mm)	Total Reading, M_T (µSv/5min)	SD-Total (µSv/5min)	%SD-Total	Shadow Reading, M_S (µSv/5min)	SD-Shadow (µSv/5min)	%SD-Shadow
1000	19.213	0.161	0.8	2.620	0.017	0.6
1500	9.303	0.136	1.5	2.192	0.011	0.5
2000	5.715	0.049	0.9	1.800	0.025	1.4
2500	4.104	0.055	1.3	1.581	0.035	2.2
3000	3.169	0.045	1.4	1.422	0.009	0.6
3500	2.560	0.032	1.3	1.244	0.027	2.1
4000	2.092	0.054	2.6	1.148	0.033	2.8
4500	1.786	0.038	2.1	1.023	0.033	3.2
5000	1.546	0.020	1.3	0.926	0.035	3.8

8.3 Shadow Shield Method in ISO 10647 Standard

8.3.1 Characteristic Constant, k

The initial values of the monitor readings, corrected for air attenuation (F_A) and geometry factor (F_1) and converted to μSv/h, are listed in Table 14. The difference between corrected total and shadow readings was applied into the left-hand side (LHS) of equation (1) and plotted as a function of effective distance. The function's slope was 200.45 μSv/h. The applied parameters[2, 3] to obtain these factors are listed in Table 16.

Table 14: Total and net readings (total and shadow) of the monitor at different distances to the neutron source. The last column lists the corresponding values of the left-hand side (LHS) of equation (1).

Distance, l (m)	Total Reading, M_T (μSv/5min)	Shadow Reading, M_S (μSv/5min)	M_T (μSv/h)	M_S (μSv/h)	$1/l^2$ (m^2)	Air-Attenuation Correction $F_A(l)$	Geometry Correction $F1(l)$	LHS of Eq.1
1	19.213	2.620	230.55	31.44	1.00	1.0089	1.0014	200.56
1.5	9.303	2.192	111.63	26.30	0.44	1.0134	1.0006	86.40
2	5.715	1.800	68.58	21.60	0.25	1.0180	1.0004	47.81
2.5	4.104	1.581	49.25	18.97	0.16	1.0225	1.0002	30.95
3	3.169	1.422	38.03	17.06	0.11	1.0271	1.0002	21.53
3.5	2.560	1.244	30.72	14.93	0.08	1.0316	1.0001	16.28
4	2.092	1.148	25.11	13.77	0.06	1.0362	1.0001	11.74
4.5	1.786	1.023	21.43	12.28	0.05	1.0409	1.0001	9.53
5	1.546	0.926	18.55	11.11	0.04	1.0455	1.0001	7.77

The Characteristic Constant (k) corresponded to the slope of the fitted linear function of LHS values versus the squared distance. The responses of the fluence rate (R_ϕ) and the dose equivalent rate (R_H) were derived from the k value for the ICF monitor. The calibration factor (C_F) of the monitor (i.e. the reciprocal of the response) was also calculated. The obtained parameters at 1 metre are also listed in Table 16.

There was a 14 percent difference between the free field dose rate response = 233.22 μSv/h per $n.m^2$ and the measured one. Consequently, the correction factor (C_F) for the ICF monitor should be the ratio of the free field (i.e. the source certificate) to the measured values. This factor represents the *in situ* calibration factor of the monitor.

$$\mathbf{C_F = 233.22 / 200.45 = 1.16}$$

Table 15: The values of measured k and the certificate's free field for the ICF reference monitor at 1 metre. This k constant characterised the monitor, the neutron source and the calibration room as one system. R_ϕ is the free field fluence response.

Distance, ℓ (m)	Characteristic Constant, k (μSv/h	Dose Rate Response of free field, R_H (μSv/h)	Difference%, k to R_H	Calibration Factor, C_F (μSv/h) per (nominal μSvs/h)	Ratio of Measured to Free Field Responses (nominal μSv/h) per (μSv/h)
1	200.45	233.22	14	1.16	0.86

The relationship between k value and the corrected reading[3] 'M_c' is given in equation (15). The monitor reading must be corrected for all extraneous effects to obtain 'M_c' in equation (1). The k value must also be traceable to a recognisable standard authority e.g. PTB[†], NPL[‡] etc.

(15) $$\mathbf{k = M_c \,.\, \ell^2}$$

A plot of LHS values of equation (1) versus squared distances is given in Figure 3. The slope of linearly fitted data was 200.4 μSv/h, which corresponded to the Characteristic Constant (k) per neutron fluent rate for the ICF. The fitted function is given by:

$$\mathbf{y = 200.4\ x - 0.915}$$

Where:

'y' and 'x' represent the corrected monitor reading (M_c) and the inverse of the squared distance ($1/\ell^2$) respectively.

[†] Physikalisch-Technische Bundesanstalt, Germany.
[‡] National Physical Laboratory, UK.

Figure 3: The Characteristic Constant plot using data in the Table 14. The LHS values plotted versus the inverse of squared distance. The slope of the straight line represents the value of Characteristic Constance (k) of equation (1). R^2 represents the correlation factor of the linearly fitted data.

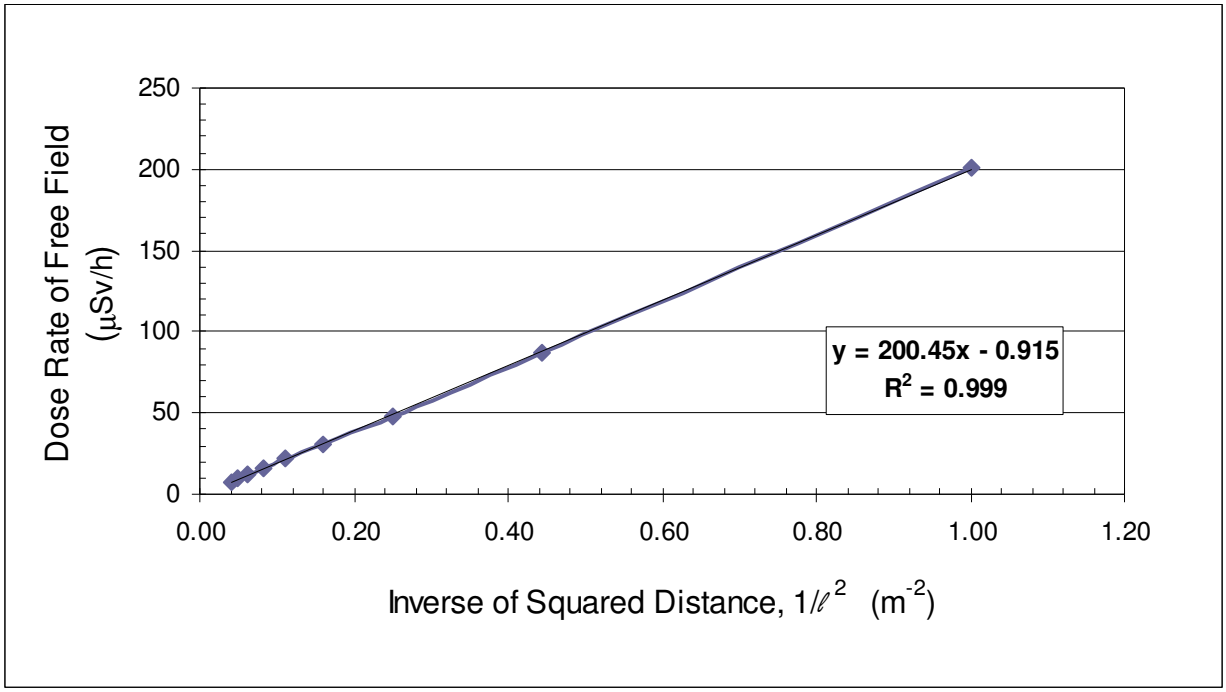

The linear fitting was found to have a good correlation factor, $R^2 = 0.999$. Nevertheless, the line intercepts the 'y' axis at 0.915 uSv/h, which has a slight offset from the ISL in equation (1). This offset must be included when this function is applied in operational client calibrations i.e. it must be subtracted from the reading.

Table 16: Summary of factors used to convert fluence to dose equivalent or dose rate equivalent. It also includes the parameter which is applied to obtain the correction values of geometry and scatter effects for the LHS of equation (1).

Neutron Effective Parameter, (δ)		0.5
Total Air Scatter per metre		0.009
Fluence to Dose Conversion Factors	Sv/cm^2	3.91E-10
	Sv/m^2	3.91E-14
	$\mu Sv/m^2$	3.91E-08
ICF Free Field Dose Rate equivalent at 1m	μSv/h	233.22

8.3.2 Performance Test of LiBr Shadow Shield

The linear relation in Figure 3 illustrated a good agreement between the inverse square law (equation 1) and the free field response of reference monitor at the ICF calibration room. This result was considered as good indication of the functional integrity and satisfying performance of the constructed LiBr shadow shield.

8.4 Semi-Empirical Method in ISO 10647 Standard

Table 17 lists the measured total readings and the corresponding values generated by this technique's equation (3) in method section 3.2. Values of the left-hand side (LHS) of the equation were listed in column four. These values were corrected for relevant geometry as

well as total air scatter effects. The latter factor is equal to the inscatter minus the outscatter components. These correction factors used in the equation were listed in column six and eight.

Figure 4 shows a plot of the LHS values (measurements) versus squared distance (ℓ^2) as well as their linearly fitted function. The linear fitting is given in equation (16) with a correlation factor of $R^2 = 0.97$. The variables 'y' and 'x' in the equation represent the corrected value of the total reading of the ICF reference monitor and the squared distance of source to monitor respectively.

(16) **y = 5.879e-6 x + 1.439e-4**

The maximum deviation from linearity was within three percent. This deviation shall be included as an error when equation (16) is utilised in operational calibration of similar monitors. This equation was rearranged to obtain the fractional room return scatter (S) = 0.041 and the fluence rate response=1.439e-4 (monitor reading per n/m^2). The resulted new format is given in equation 17. This S value agreed with the that obtained by NCRP 112 method with 93.2% (S = 0.044, section 8.6.2).

(17) **y = 1.439e-4 (1+ 0.041 x)**

Hence, the corresponding monitor reading, induced by the free field of ICF neutron fluence (i.e. 1.657e6 n/m^2) at 1 metre, was calculated as follows.

Monitor Reading =1.439e-4 x 1.657e6 = 238.44 µSv/h

This response of the ICF reference monitor must be traced to an acceptable standard authority e.g. PTB[§], NPL[**]…

Table 17: Monitor readings (LHS of equation 3) and the applied correction values of air scatter and geometry at different distances between the neutron source and monitor.

Distance, ℓ (m)	Total Reading (µSv/5min)	Total Reading, M_T (µSv/h)	LHS of Eq.3 (µSv/h per n/m^2)	ℓ^2 (m^2)	Air-Inscatter, $(1+A^*\ell)$	Fluence (n/m^2)	Geometry Factor, $F_1(\ell)$
1	19.213	230.554	1.38E-04	1.00	1.009	1.657E+06	1.0014
1.5	9.303	111.631	1.49E-04	2.25	1.0135	7.364E+05	1.0006
2	5.715	68.585	1.63E-04	4.00	1.018	4.142E+05	1.0004
2.5	4.104	49.248	1.82E-04	6.25	1.0225	2.651E+05	1.0002
3	3.169	38.028	2.01E-04	9.00	1.027	1.841E+05	1.0002
3.5	2.560	30.718	2.20E-04	12.25	1.0315	1.353E+05	1.0001
4	2.092	25.109	2.34E-04	16.00	1.036	1.036E+05	1.0001
4.5	1.786	21.432	2.52E-04	20.25	1.0405	8.182E+04	1.0001
5	1.546	18.550	2.68E-04	25.00	1.045	6.627E+04	1.0001

[§] Physikalische-Technische Bundesanstalt (PTB) in Germany.
[**] National Physical Laboratory in UK.

Figure 4: Plot of the semi empirical method results given in Table 17 (fourth and fifth columns). LHS values were plotted versus the corresponding squared distance (ℓ^2). The data were also fitted into a linear function of correlation factor $R^2 = 0.97$.

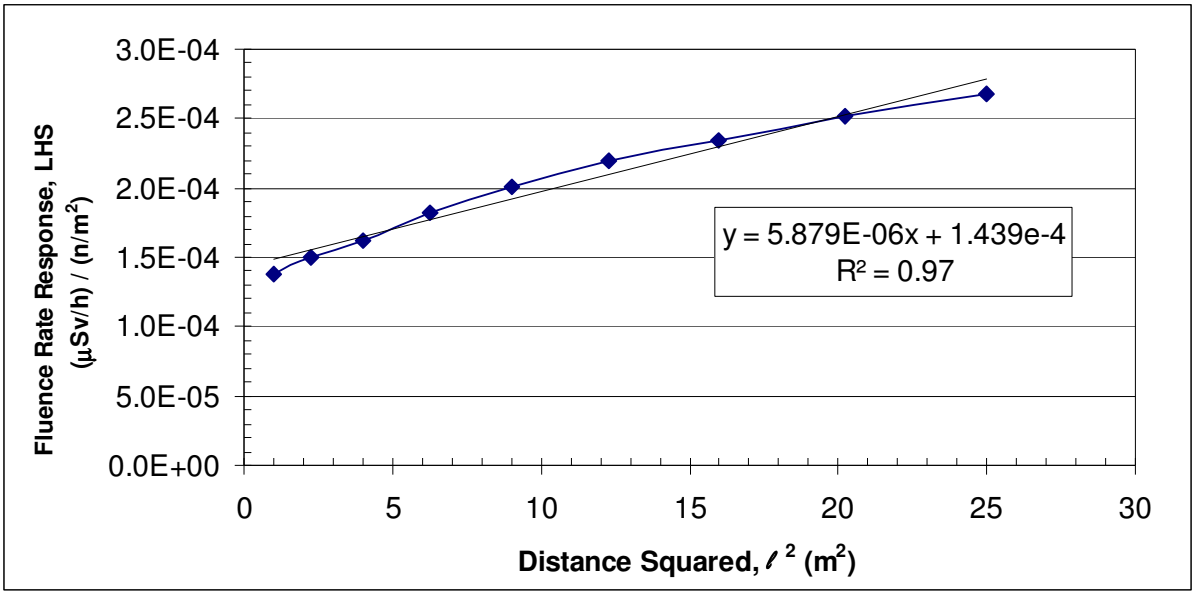

ISO 10647 standard[3] recommends that the scatter component in a neutron-calibration field should not exceed 40 percent. Thus, the obtained S value of the ICF calibration room was translated to a maximum calibration distance (ℓ) = 3.12m. The details of calculations are provided below:

S x ℓ^2 should be less or equal 40%
0.041 x ℓ^2 =<40/100
ℓ = √ (0.4/0.041) = 3.12m

A summary of the obtained values by the semi empirical method of ISO 10647 standard is shown in Table 18 below.

Table 18: The Fractional Room Return Scatter at the ICF calibration room, obtained by using the ISO 10647 Semi Empirical method. Also listed are the *in situ* calibration factor (C_F), the fluence and dose rate responses of the ICF reference monitor.

Fluence Response, R_ϕ [Measured] (µSv/h) per(n/m²)	C_F (µSv/h) per (Nominal µSv/h)	Response of Dose Rate Equivalent, R_H (Nominal µSv/h) per (µSv/h)	Fluence Rate Response, hϕ [reference] (µSv/h/m²)	Fractional Room Return Scatter, S
1.439E-04	0.98	1.02	1.41E-04	0.041

8.5 Polynomial Fit Method in ISO 10647 Standard

The measurement results by this method are listed in Table 19. The values of left hand side of equation (4), listed in column six, were obtained by dividing the total reading (M_T) over the product of neutron fluence and geometry factor, $F_1(\ell)$. These values were then fitted into a second degree polynomial function to determine the function's coefficient constants.
The RHS values were generated from the characterised polynomial function, which represented the predicted responses of ICF reference monitor versus distances. Obviously, the correction for total air scatter effect, i.e. inscatter minus outscatter, was incorporated within the polynomial coefficients.

The data provided in bold font was used in the polynomial fitting assessment using the Power Matrix LSM.

Table 19: A list of total readings and the relevant generated values of RHS of equation (4) of the polynomial technique given in 3.3. The data provided in bold was used in the polynomial fitting assessment of Power Matrix LSM.

Distance, ℓ (m)	ℓ^2 (m^2)	Total Reading, M_T (μSv/h)	Geometry Factor, $F_1(\ell)$	Fluence (n/m^2)	LHS (μSv/h per n/m^2)	RHS (Forsythe Analysis)	%Δ of RHS to LHS
1	**1**	**2.306E+02**	**1.0014**	**1.657E+06**	**1.389E-04**	**1.360E-04**	**2.09**
1.5	2.25	1.116E+02	1.0006	7.364E+05	1.515E-04	1.526E-04	-0.75
2	**4**	**6.858E+01**	**1.0004**	**4.142E+05**	**1.655E-04**	**1.697E-04**	**-2.51**
2.5	6.25	4.925E+01	1.0002	2.651E+05	1.857E-04	1.872E-04	-0.77
3	**9**	**3.803E+01**	**1.0002**	**1.841E+05**	**2.065E-04**	**2.051E-04**	**0.69**
3.5	12.25	3.072E+01	1.0001	1.353E+05	2.271E-04	2.235E-04	1.58
4	**16**	**2.511E+01**	**1.0001**	**1.036E+05**	**2.424E-04**	**2.424E-04**	**0.04**
4.5	20.25	2.143E+01	1.0001	8.182E+04	2.619E-04	2.617E-04	0.10
5	**25**	**1.855E+01**	**1.0001**	**6.627E+04**	**2.799E-04**	**2.814E-04**	**-0.55**

8.5.1 Forsythe Orthogonal Fitting

The values of LHS were fitted into a second degree polynomial function versus distance (ℓ) to determine the function coefficient constants using the Forsythe Orthogonal Method (Figure 5). The resulted polynomial function was rearranged in order to determine the fluence rate response (h_ϕ), i.e. to match the same format given in equation (5). Both function's forms are given below, where 'x' represents the distance (ℓ) and 'y' represents the RHS value.

$$\mathbf{y = 1.042e\text{-}4 + 3.092e\text{-}5\ x + 9.038e\text{-}7\ x^2}$$

or

$$\mathbf{y = 1.042e\text{-}4\ (1 + 2.966e\text{-}1\ x + 8.671e\text{-}3\ x^2)}$$

From the above equation, the fluence response (R_ϕ) for the ICF reference monitor (*in situ*) corresponded to 1.042e-4 (monitor reading per n/m^2). Furthermore, the corresponding value of the monitor reading that was induced by the free field of the ICF neutron fluence (i.e. 1.657e6 n/m^2) at 1 metre was calculated as follows.

Monitor Reading =1.042e-4 x 1.657e6 = 172.66 μSv/h

The dose rate equivalent response (R_H) in column five of Table 20 was derived from the ratio of the monitoring reading to the corresponding value of the free field dose rate at the ICF (233.2 μSv/h).

8.5.2 Power Matrix Fitting

Initially, the power matrix Least Square Method[12,14,22] (LSM) was tried to fit all measurement data. However, it could not handle more than five data points, i.e. it encountered matrix singularity due to the very small value of the matrix of coefficients. Therefore five measurement data (bold values, Table 19) were then applied to derive the quadratic fitting function below. The results obtained through the LSM and Forsythe methods were very similar and only within three percent of difference. However, ISO 10647 standard[3] recommends the use of 10 or more data points for good fitting, hence the Forsythe method was adapted in this characterisation technique.

$$\mathbf{y = 1.073e\text{-}4 + 2.876e\text{-}5\ x + 1.186e\text{-}6\ x^2}$$

or

$$\mathbf{y = 1.073e\text{-}4\ (1 + 2.679e\text{-}1\ x + 1.105e\text{-}2\ x^2)}$$

The above equation gave fluence response (R_ϕ) = 1.073e-4 (monitor reading per n/ m^2) for the ICF reference monitor. Therefore, the corresponding value of the monitor reading that was induced by the free field of the ICF neutron fluence (i.e. 1.657e6 n/ m^2) at 1 metre was calculated as follows.

Monitor Reading =1.073e-4 x 1.657e6 = 178.0 μSv/h

The fluences and calibration factors, derived by both analysis methods for the ICF monitor, are listed in Table 20 below for comparison.

The dose rate equivalent response (R_H) in column five of Table 20 was derived from the ratio of the monitoring reading to the corresponding value of free field dose rate at the ICF (233.2 μSv/h).

Table 20: The obtained parameters x and y of equation (4) for the ICF reference monitor/source. The table also lists the relevant responses of fluence, dose rate equivalent, the calibration factor and the fluence rate to dose rate conversion factor.

Fluence Response, R_ϕ (μSv/h per n/m^2)	X Coefficient	y Coefficient	Fluence to Dose Rate factor, hϕ (μSv/h per n/m^2)	Dose Rate Equivalent Response, R_H (μSv/h)	Calibration Factor, C_F	poly-fit method RHS= R_ϕ.(1+x.f+y.f^2) = a+b.f+c.f^2
1.042E-04	2.966E-01	8.671E-03	1.41e-4	0.74	1.35	Forsythe
1.073E-4	2.679E-1	1.105E-2	1.41e-4	0.76	1.31	Power Matrix

Figure 5: Plots of LHS and RHS values versus distances. R^2 represents the correlation coefficient of fitted data (RHS values). The equation of monitor response as a function of distance (ℓ) is also listed.

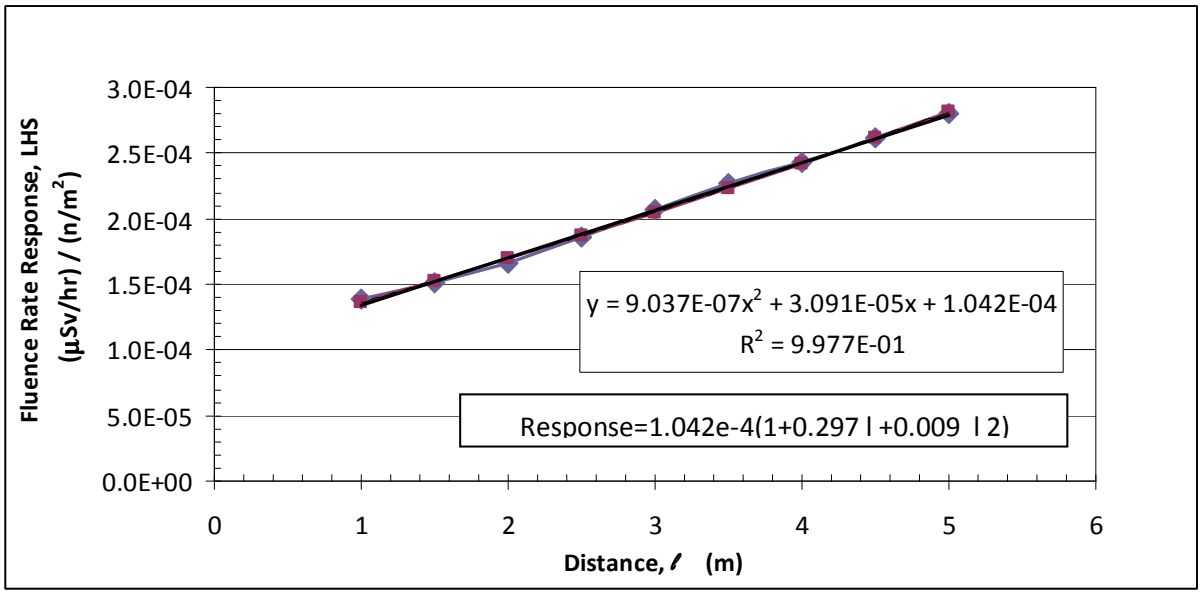

8.6 Shadow Method in NCRP[5,4] 112 Report

8.6.1 Fractional Dose Rate of Free Field Neutrons

The component of direct neutron fluence, impinging on the monitor, was deduced by taking the difference between the Total and Shadowed readings. The fractions of direct dose rates are the ratio of direct to the total readings as a function of corresponding distances and are listed in Table 21. The fractional dose rates and their associated combined standard deviations (SD) were also listed. The error propagation formula[15,16,17] was applied to obtain the combined standard deviation. A plot of these fractions versus distances (ℓ) is illustrated in Figure 6.

The air scatter correction factor was neither applied to the total nor to the 'direct' readings because it would cancel out as a reading ratio.

Table 21: Values of dose rate fractions of free field neutrons (direct) at the ICF calibration room. These fractions represented the ratio of direct to total doses recorded by the ICF reference monitor at various distances (ℓ). The SD represents the combined statistical standard deviation.

Distance, ℓ (m)	Total Reading (µSv/5min)	Shadow Reading (µSv/5min)	Readings Difference (µSv/5min)	SD of Difference (µSv/5min)	Fraction of Direct Dose Rate	SD of Fraction	%SD of Fraction
1	19.213	2.620	16.593	0.162	**0.864**	0.011	1.3
1.5	9.303	2.192	7.111	0.136	**0.764**	0.018	2.4
2	5.715	1.800	3.916	0.055	**0.685**	0.011	1.6
2.5	4.104	1.581	2.523	0.065	**0.615**	0.018	2.9
3	3.169	1.422	1.747	0.046	**0.551**	0.016	3.0
3.5	2.560	1.244	1.316	0.042	**0.514**	0.017	3.4
4	2.092	1.148	0.945	0.063	**0.451**	0.032	7.2
4.5	1.786	1.023	0.763	0.050	**0.427**	0.029	6.9
5	1.546	0.926	0.620	0.040	**0.401**	0.027	6.6

A linear regression function 'y' was also fitted to the data and plotted. It was evident that this function demonstrated a fair correlation coefficient R^2 = 0.964. However, the noticeable deviation of data points at both ends of the fitting indicated a higher departure of the total air scatter from the linear trend assumption. At the shorter distance, this departure could be caused by an insufficient air gap between the shield and monitor; whereas, at the longer distance it could be caused by the dominant scatter component and the shift of average energy of the source's neutron spectrum.

The linear and quadratic functions described the fractional dose rate versus distance (in metres) are given below. The 'y' and 'x' represent the fractional dose rate and distance respectively; R^2 is the correlation coefficient of fitting:

$$\mathbf{y = - 0.114\ x + 0.929} \qquad \mathbf{; R^2 = 0.964}$$

$$\mathbf{y = 0.019\ x^2 - 0.229\ x + 1.069} \qquad \mathbf{; R^2 = 0.998}$$

The deviation from the linear function should be included as error values in operational calibration.

Figure 6: The fractional direct dose rate versus distance (ℓ) at the ICF calibration room. The data fits a quadratic function (red curve) with a correlation coefficient R^2= 0.999. The straight line represents the data's linear fitting for comparison with a correlation coefficient R^2= 0.964.

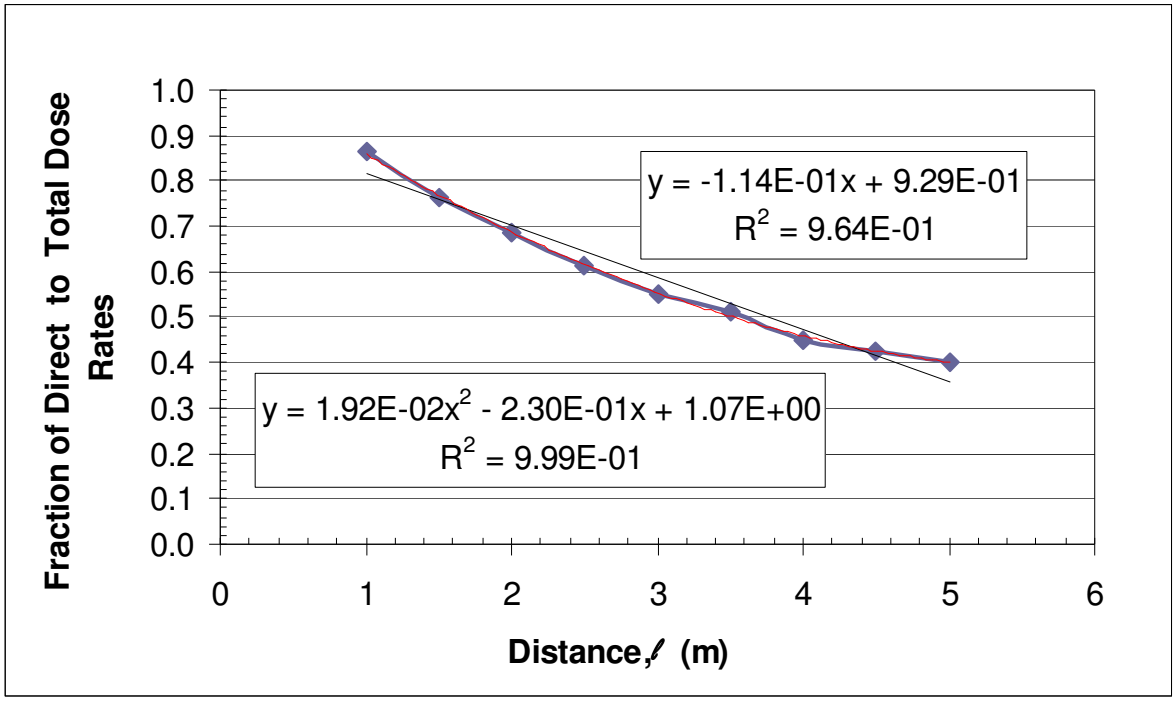

8.6.2 Fractional Room Return Scatter

The measurement data in column five were corrected for geometry (F_1) and air attenuation (F_A) effects and listed in column seven of Table 22. Data in column seven were linearly fitted as a function of values in column three to obtain the equation (**18**) of monitor response.

(18) $$y = 240.21 + 10.531x$$

The above equation was rearranged in line with equation (5) (in the method section 3.4) to determine the monitor response (D_0) and the fractional room return scatter (S).

(19) $$y = 240.21(1 + 0.044x)$$

Where:

y represents the $D.\ell^2$

x represents the squared distance (ℓ^2)

The fractional room return scatter (S) and the response (D_o) of dose rate were then determined from the parameters of the above equation at 1 metre exclusive distance between source and monitor. Their values were:

D_o value = 240.21 (μSv/h per n/m^2)

S value = 10.531 / 240.21 = 0.044 at 1m in ICF calibration room.

A plot of the equation is shown in Figure 7. Nevertheless, both S and D_0 values must be linked to a recognisable standard authority e.g. PTB, NPL...

Table 22: Monitor total readings at various source-monitor distances. Data in columns three and seven were fitted into a linear function to derive the room return scatter (S) and dose rate response (D_o at 1 metre) in the ICF calibration room. F_A and F_1 are the correction factors of total air attenuation and geometry respectively.

Distance, ℓ	Total Reading, (M_T)	ℓ^2	($M_T.\ell^2$)		($M_T.\ell^2$)x(F_A/F_1)	
(m)	(μSv/5min)	(m^2)	(μSv/5min).m^2	(μSv/h).m^2	(μSv/5min)	(μSv/h)
1	19.213	1	19.213	230.556	19.357	232.284
1.5	9.303	2.25	20.931	251.172	21.199	254.388
2	5.715	4	22.862	274.344	23.264	279.168
2.5	4.104	6.25	25.650	307.800	26.221	314.652
3	3.169	9	28.521	342.252	29.288	351.455
3.5	2.560	12.25	31.358	376.296	32.346	388.152
4	2.092	16	33.478	401.736	34.689	416.268
4.5	1.786	20.25	36.167	434.004	37.642	451.704
5	1.546	25	38.645	463.740	40.401	484.812

The plots of corrected data and fitted function are illustrated in Figure 7. These data (column seven) are plotted versus squared distances (ℓ^2) (column three). The value of monitor's fluence response (D_o) and the fractional room return scatter (S) were derived from the coefficients of the fitted linear function i.e. equation (**19**).

The values in column six were multiplied by 12 (i.e. minutes to hour factor, (60 min/h) / 5 (min)) to converted them to the common unit of dose rate response i.e. (μSv/h), which listed in column seven.

This D_o value (240.2 μSv/h) was then compared with the corresponding free field i.e. value = 233.2 μSv/h of the ICF source (detailed in section 8.1). The difference percentage (Δ%) between these values was found to be minimal.

$$\Delta\% = [(233.2 - 240.2)/233.2]x100 = -3\%$$

A summary of the S and D_0 values, obtained by the NCRP 112 method is given in Table 23.

Table 23: Values of S and ($D_0 = R_\phi$), obtained by the NCRP 112 method. 'Δ%' represents the percentage difference between the monitor response and the free field fluence rate of the ICF neutron source. The measured response represents the value that was obtained from the fitted linear function.

Room Scatter Factor, S	Measured R_ϕ (µSv/5min)	Measured R_ϕ (µSv/h)	Calculated R_ϕ (µSv/h)	Δ%Source to Direct Dose Rates
0.044	20.018	240.216	233.2	-3

Figure 7: Plot of room return scatter: the product of the total reading by squared distance ($D.\ell^2 = M_T.\ell^2$) versus the squared distance (ℓ^2). The linear fitting has a correlation coefficient $R^2 = 0.976$.

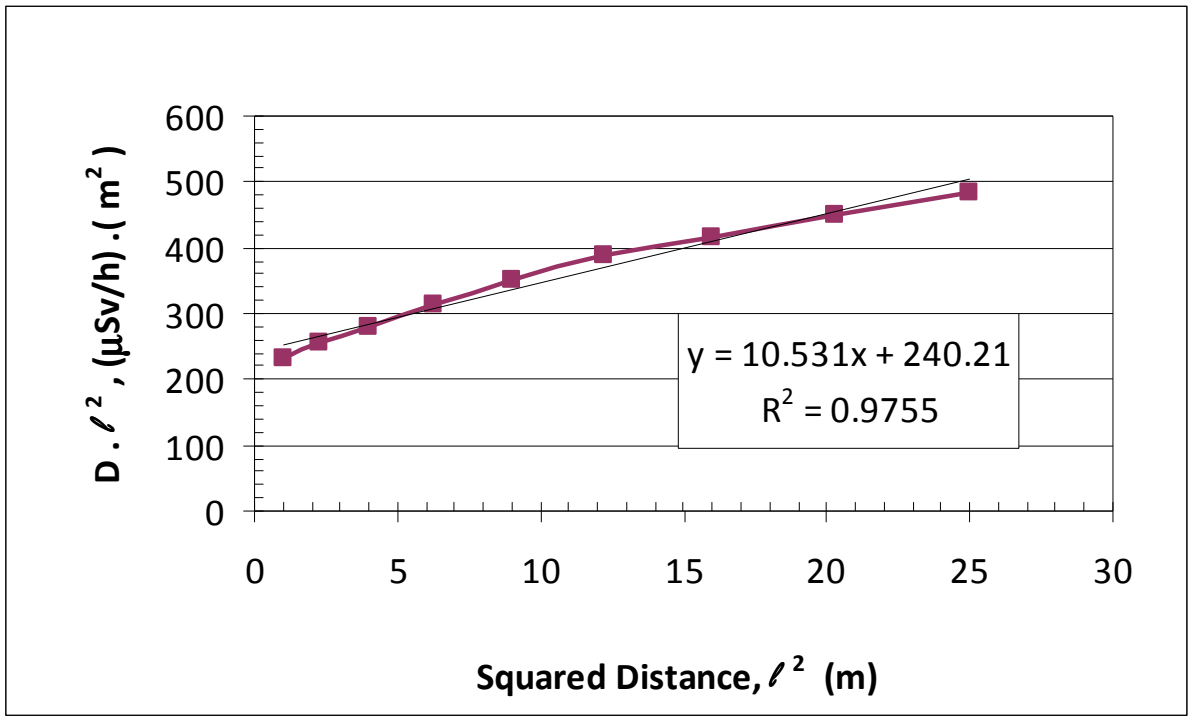

The ISO 10647 standard[3] recommends that the scatter component in a neutron-calibration field should not exceed 40 percent. This scatter, as a function of distance, is given by the following equation:

$$S \times \ell^2 =< 40\%$$

Thus, the maximum distance (ℓ) at the ICF rig calibration room that would fulfil this requirement was calculated as follows.

$$0.044 \times \ell^2 =< 40/100$$

Hence,

$$\ell = \sqrt{(0.4/0.044)} = 3.02m$$

8.7 Summary of Fractional Room Return Scatter and Monitor Response

The measured fractional room return scatter S that characterised the ICF calibration room, using the ICF reference monitor and neuron source of serial number 4232 NE, is listed in column three of Table 24. The standards and methods which were applied to determine the S value are listed in columns one and two.

Table 24: Measured values of the fractional room return scatter (S) at the ICF calibration room. The applied standards and methods are also listed.

Standard	Method	*Fractional Room Return Scatter, S*
NCRP 112	$D.\ell^2 = D_o.(1 + S.\ell^2)$	*0.044*
ISO 10647	Semi-Empirical	*0.041*
ISO 10647	Shadow Shield	n/a (incorporated within the Characteristic Constant k)
ISO 10647	Polynomial	n/a

Table 25 lists a summary of the measured responses at 1 metre by the ICF reference monitor and the applied standards and methods of measurements and analysis.

The values of fluence response in column six were obtained by dividing the monitor reading (column four) by the neutron fluence (1.657e6 n/m^2) of free field at 1 metre in the ICF calibration room (section 8.1). The values of monitor 'reading' in column four were obtained from the fitted equation of the corresponding method. They included the corrections of air attenuation and geometry effect when appropriate; the fluence response was multiplied by the ICF neutron fluence to obtain the monitor reading in column four.

The bolded values in column four were adopted and will be applied in the operational calibration procedures.

The calibration factors (C_F), shown in column six, were obtained by dividing the ICF free field dose rate at 1metre (i.e. 233.2 μSv/h) by the corresponding values of monitor reading given in column four. These factors represented the *in situ* values and must be linked to a recognisable standard authority for traceability e.g. PTB, NPL...

Table 25: Summary of measured monitor responses at 1 metre by the ICF reference monitor. Also listed are the applied standards, methods and fitting analysis. The *in situ* calibration factors (C_F) of the ICF reference monitor are shown in the last column.

Standard	Methods		Monitor Reading @1m (μSv/h)	Fluence Response (nominal μSv/h) per (n/m^2)	Calibration Factor, C_F (μSv per nominal μSv)
	Measurement	Analysis			
NCRP 112	$D.\ell^2 = D_o.(1 + S.\ell^2)$	Forsythe	**240.12**	1.449E-04	0.97
ISO 10647	shadow	Forsythe	**200.40**	1.210E-04	1.16
ISO 10647	semi-empirical	Forsythe	245.24	1.480E-04	0.95

ISO 10647	semi-empirical	Excel 97	238.44	1.439E-04	0.98
ISO 10647	polynomial	10 points Forsythe	172.66	1.042E-04	1.35
ISO 10647	polynomial	5 points Power Matrix	178.0	1.073E-04	1.31
Reference Values:					
fluence to dose conversion factor at ICF, [µSv/h per n/m^2]			Section 8.1		1.407e-4
fluence to dose conversion factor at ICF, [n/m^2 per µSv/h]			1/1.407e-4		7.104e+3
ICF free field fluence at 1m, [n/m^2]			Section 8.1		1.657e+6
ICF free field dose rate at 1m [µSv/h]			Section 8.1		233.2

9 Discussion

An aqueous LiBr shadow shield (cone) was designed and constructed. The properties of involved materials were evaluated e.g. neutron absorption and scattering. The geometry, described in the NCRP 112 Report, was adopted in this design. Also, the evaluation included the comparison of neutron diffusion length between LiBr and Li_2CO_3 compounds.

The deviation from the construction and utilisation of the Li_2CO_3 wax cone, as described in the report, was prompted by the technical difficulties and poor quality of the initial manufactured cone (e.g. non uniformity of neutron absorber particulates, air voids, time constrain and manufacturing delay…).

The evaluation (detailed in section 5.2) showed that the cone with the LiBr compound possessed seven percent higher absorption and 31 percent less scatter cross sections to neutrons, compared with the Li_2CO_3 cone. Consequently, the LiBr cone should cause less scattering and more absorption to the direct impinging neutrons than the Li_2CO_3 cone (advantage). Furthermore, the higher absorption feature reduces the available direct neutrons for scattering.

In addition water (as solvent) possesses a short Diffusion Length[23] (L = a few centimetres) and therefore the majority of the scattered neutrons would take place within the solution and eventually be absorbed with minimal additional scatter outside the cone. The presence of C and O atoms in the moderating materials (water or wax) of both cone types should have insignificant effects due to their very large L values.

It was found that the alternative shadow shield with the LiBr solution had several advantages such as ready availability, the low cost of construction materials and the simple and straightforward steps of solution reparation and cone-shell fabrication.

Performance tests carried out on the LiB aqueous shield (cone) illustrated that the direct neutron fluence (difference between total and scattered neutrons) followed the ‘inverse square law’ quite well, with a correlation factor =0.999 (see Figure 3).

The values of the fractional room return scatter (S), determined by the semi-empirical of ISO10647 and shadow shield of NRCP112, were in reasonable agreement within seven percent (see Table 24).

The size of the ICF calibration room fulfils the requirement by the shadow shield method i.e. a medium to a large size room (see appendices). Also, the fluence responses were relatively in good agreement with the calculated value from the source certificate; the resulted values of Characteristic Constant k and S, had good fitting's correlation coefficient. Therefore, these values were adopted for operational calibration services.

The S value at the ICF calibration room changes as a function of the second degree polynomial of distance. So beyond about three metres in distance the corresponding S value exceeds 40 percent of the recommended scatter limit by ISO 10647 (to avoid significant change to the neutron energy spectrum of the ^{241}Am/Be source). Notably, this distance is 90 percent of the radius between the source-guide tube and room walls (see Figure 2). This suggests that the room floor contributes more scatter than the walls. Thus a further increase in source height would reduce the floor scatter and ultimately the overall scatter (e.g. floor and walls). However, other competing factors should be carefully considered in such a decision, like the convenience of the instrument's set up, the frequency / demand for such a distance (e.g. low dose/rate), the cost to build an off ground calibration platform etc…

All parameters obtained in the ICF characterisation should be linked to a recognisable standard authority e.g. PTB, NPL…

The ICF reference monitor showed variations in the values of responses and calibration factors which were clearly dependent on the applied method. A summary of these values is provided in Table 25.

A comparison between the calibration factor (*in situ*, obtained in this work) of the ICF reference monitor with a traceable calibration by a recognisable standard authority (e.g. PTB, NPL…) of the same monitor should give an insight into the integrity of the current neutron source in the ICF rig. It also provides a practical way to validate its emission versus calibration certificate.

The values of a free field dose rate of 16.2mSv/h, 3.7mSv/h and 0.933 mSv/h, corresponding to the distances of 0.12m, 0.25m and 0.5m respectively (in Table 11), were obtained by extrapolation calculations. They will provide extra calibration capability at the ICF rig calibration room which is required by some clients. However, it should be noted that these dose rates are still well below the upper-end of the recommended[3] dose rate by the ISO 10647 standard (i.e. 40mSv/h for neutron calibration facility, radiological applications).

The standard also recommends 10μSv/h at the lower-end of dose rate range. Such a dose rate would be achieved at distance of about 5 metres in the ICF rig calibration room. However, this distance is beyond the maximum distance limit for 40 percent of scattered neutrons and should be avoided.
In order to comply with the standard an alternative solution would be the installation of two neutron sources in the ICF rig. Their activities shall be carefully chosen to provide the recommended dose rates within the recommend distance range[3] i.e.=<40% scattered neutrons.

Different fitting methods illustrated a slight effect on the coefficients of fitted quadratic equations, which mainly affects the monitor response value (see Table 25). Overall, all fitting methods give comparable linear results (about four percent).

Equations linearly fitted by Forsythe or Excel data analysis technique gave comparable results.

The calibration stand, attached to the moving rail, was wobbly and shall be rectified; the vertical deviation must not exceed 2mm.

The arithmetical mean and sample standard deviation (SD) of five repeated measurements were used to represent the average reading and its associated statistical dispersion. The uncertainty propagation technique was applied to obtain the combined uncertainty (A type) of a given measurement technique's function.

The agreement of fitted functions with the hypothesis of the measurement analysis was considered as an illustration of good accuracy with measurement[16]. Furthermore the accuracy of linear slope, used to obtain the monitor response, should be verified with the corresponding traceable value of monitor response (when available).

A Maximum Likelihood Test[16] (χ^2 Parameter) would provide an index of accuracy between the hypothesis and measurement but would require a large set of data and counts which was not possible to apply to this work due to time constraints. The uncertainty scope given in ISO 10647 is still applicable to this work and should be considered as Type B[15,17].

Recording devices for temperature, pressure and humidity should be installed in the ICF calibration room. Additional shadow shields of smaller sizes are required to characterise different geometries.

It is recommended to explore an appropriate mechanism / adaptor fitting at the top of the source-tube, so the anisotropy check of the source can be carried out easily and regularly for QA fulfilment.

It is worth noticing that at the completion of this characterisation and report, the calibration results with the Physikalische-Technische Bundesanstalt (PTB) in Germany became available. As a result, the neutron characterisation at ICF calibration room did agree with the BTP calibration within five percent. Consequently, the neutron field in ICF rig calibration room is now traceable to BTP standard laboratory in Germany. Also, this agreement confirms the integrity of the current neutron source e.g. anisotropy stability, which should save substantial cost and efforts in replacing the source or sending it overseas for re-certification.

The details of the results comparison as well as copy of the PTB calibration report are given in appendices 11.3 and 11.4.

10 Conclusions

- The Fractional Room Return Scatter (S) at the ICF calibration room was determined. The small S value illustrated a good quality feature of the room.
- The measured S Values by NCRP112 or ISO10647 methods were in good agreement (93 percent).
- Operational calibrations should be carried out within three metres distance from the neutron source in order to comply with 40 percent of the room scatter limit; recommended by the ISO 10647 standard[3].
- The new type of aqueous LiBr truncated cone was successfully implemented in measurements by the shadow shield technique.
- The fluence and dose rate equivalent responses (*in situ*) were determined for the ICF reference monitor. The reference neutron fluence was taken from the source certificate. Hence, the responses must be linked to a recognisable standard authority e.g. PTB, NPL… for legal traceability requirements.
- Three extra positions of relatively high dose rates were determined. They will expand the capability of dose rate range at the ICF calibration service that are desired by some clients.
- The reference neutron fluence given in the source's certificate should be compared with the corresponding value provided by the standard authority as a measure of the source's integrity at the rig calibration room.
- The characteristic parameters measured by the different techniques were evaluated and the appropriate ones identified for implementation at the ICF calibration room. Furthermore the relevant operational instructions should be developed for future routine calibrations.
- The facility currently lacks a high dose rate range (recommended[3] by the ISO 10647 Standard) that is usually available at similar facilities.
- The ICF should have two neutron sources of appropriate activities to achieve the recommended[3] dose rate range.
- Additional shadow shields are required for other characterisation geometries in future.
- The neutron field at ICF rig room becomes now traceable to the Physikalische-Technische Bundesanstalt (PTB) in Germany. The calibration result by this standard authority became available after the completion of this characterisation and report. ICF results did agree with PTB calibration within five percent.

11 Appendices

11.1 Advantages of Different Techniques

Shadow Cone	Semi-Empirical	Polynomial fit
Direct measure of scatter	Direct measure of scatter	Not applicable
Any room shape	Small cubical room	Any room shape
Large room	Small room, 2mx2mx2m	Medium to large
Any source-detector distance while scatter<40%	Any source-detector distance while scatter<40%	Any source-detector distance while scatter<40%
Small source or detector size	Any size of source or detector	Large detectors or sources
Individual source	Individual dosimeter on phantom	Multi-detectors or dosimeters on phantom

11.2 Limitations of Different Techniques

Shadow Cone	**Semi-Empirical**	**Polynomial Fit**
Cone-position dependency	Non cubical room shape	Coefficients have no physical significance
Small room size	Large room i.e. >2mx2mx2m	Small room size
Large source or detector size	-	Non-linear or drift reading masked by fitting.
Distance < 2 x cone's length	Distance >= (source + detector diameter)	Distance >= (source + detector diameter)
Multi-detectors or dosimeters on phantom	Multi-detectors	-
Scatter > 40%	Scatter > 40%	Scatter > 40%
Additional set of shadow measurements	-	-

11.3 Comparison of ICF Characterisation with PTB Calibration

The *in situ* calibration factor (C_F) of ICF reference neutron monitor was 1.16 (μSv/h) per nominal (μSv/h). This factor was obtain by the shadow shield method (ISO 10647 standard) and the data of the ^{241}Am/Be source certificate[20] (4232NE; 1982; NPL Reference N113).

The PTB[††] calibration report provided three factors, applicable to the ICF reference neutron monitor. They are the calibration factor N, the linearity correction factor (k_l) and the field-specific correction factor (k_s). They are listed in tables 3 and 4 of section 11.4. A copy of the report is also shown in the section.

The relevant values of these factors were multiplied to derive the overall calibration factor (C_{ov}) for the combination of the ICF reference monitor and the neutron source i.e. ^{241}Am/Be. Also, the average (k_l (avg) of the four k_l values were applied in this calculations in order to take into account the wide range of dose rates at ICF calibration hall.

k_l (avg) = (0.999 +1+1.016+1.02) / 4
k_l (avg) = **1.009**

The applied values of these factors were N = 1.052, k_l = 1.009 and k_s = 1.04; and their details are included in the PTB calibration report. Thus, value of C_{ov} was derived as follows.

$C_{ov} = N \cdot k_l (avg) \cdot k_s$
C_{ov} = 1.052 x 1.009 x 1.04
C_{ov} = 1.104

Furthermore, the ratio percentage of PTB to ICF factors was calculated as follows.

$(C_{ov} / C_F) \times 100 = (1.104 / 1.16) \times 100 = 95.2\%$

This ratio demonstrated a good agreement of *in situ* ICF calibration with the external calibration result by the reputable standard authority, PTB.

[††] Physikalische-Technische Bundesanstalt (PTB) in Germany.

11.4 PTB Calibration Certificate of ICF Reference Monitor

Physikalisch-Technische Bundesanstalt

Braunschweig und Berlin

PTB

Kalibrierschein

Calibration Certificate

Gegenstand: *Object:*	Neutron ambient dose equivalent meter
Hersteller: *Manufacturer:*	Wedholm Medical AB Blommenshovsvägen 26 SE-61129 Nyköping
Typ: *Type:*	Neutron Monitor 2222A
Kennnummer: *Serial number:*	2222.0178
Auftraggeber: *Applicant:*	ANSTO Australia
Anzahl der Seiten: *Number of pages:*	7
Geschäftszeichen: *Reference No.:*	6.5-01/10
Kalibrierzeichen: *Calibration mark:*	64002/10
Datum der Kalibrierung: *Date of calibration:*	2010-03-11 to 2010-03-12

Im Auftrag:
By order:

Dr. A. Zimbal

Braunschweig, 2010-03-22

Siegel
Seal

PHYSIKALISCH-TECHNISCHE BUNDESANSTALT 15

Bearbeiter:
Examiner:

S. Koch

391 00B k

Kalibrierscheine ohne Unterschrift und Siegel haben keine Gültigkeit. Dieser Kalibrierschein darf nur unverändert weiterverbreitet werden. Auszüge bedürfen der Genehmigung der Physikalisch-Technischen Bundesanstalt.
Calibration certificates without signature and seal are not valid. This calibration certificate may not be reproduced other than in full. Extracts may be taken only with permission of the Physikalisch-Technische Bundesanstalt.

1. Measurement conditions

The measurements were performed free in air in a low scattering room (7 m x 7 m x 6.5 m) of the PTB in a height of 3.25 m above the floor. For the calibration with neutron radiation the reference fields from a ^{241}Am-Be(α,n)-, a ^{252}Cf- and a D_2O moderated ^{252}Cf-neutron source are available /1/. A shadow object was used for the separation of the direct and the inscattered radiation /2/.

The centre of the moderator cylinder was defined as the reference point of the instrument. The radiation incidence was perpendicular to the axis of the cylinder. Relative to the irradiation direction (from the source to the instrument) the electronics was at the right side. For the measurements the instrument was adjusted with its reference point at the test point in the radiation field.

The measurements were performed with a measuring time of 100 s. The reading quantity was the integrated dose. The dose rates were calculated from the differences of the integrated doses for intervals of 100 s. All measuring values are mean values of 10 up to 16 independent readings.

During the measurements the stability of the instrument reading was tested by a ^{241}Am-Be(α,n)-check source of the PTB. The check source was reproducibly fixed close to the surface of the instrument.

The temperature in the measuring room was between 19 °C and 21 °C, the relative humidity was between 40 % and 45 %.

2. Measurement quantity

The measurement quantity is the neutron ambient dose equivalent rate $\dot{H}^*(10)$. The conventional true value of this quantity in the irradiation fields used was calculated from the flux density of the direct neutrons, which reach the point of test without further interactions, and the fluence-to-dose equivalent conversion coefficients $h^*_\Phi(10)$. The values of $h^*_\Phi(10)$ for ^{252}Cf and ^{241}Am-Be(α,n) are taken from ref. /3,4/. The value for the moderated source takes into account that the PTB-moderator differs slightly from the ISO-moderator /5/. The fluence-to-dose equivalent conversion coefficients used are listed in table 1.

Tab. 1: Fluence-to-dose equivalent conversion coefficients

source	conversion coefficient $h^*_\Phi(10)$ pSv·cm^2
$^{252}Cf(D_2O)$	110 ± 7
^{252}Cf	385 ± 8
^{241}Am-Be(α,n)	391 ± 8

The uncertainty stated is the expanded uncertainty obtained by multiplying the standard uncertainty by the coverage factor $k = 2$. It has been determined in accordance with the "Guide to the Expression of Uncertainty in Measurement" (ISO, 1995). Normally, the value of the measurand lies within the assigned range of values with a coverage probability of approximately 95 %.

3. Determination of neutron ambient dose equivalent rate

In a given radiation field, the neutron ambient dose equivalent rate $\dot{H}^*(10)$ is derived from the instrument's reading by the following relationship:

$$\dot{H}^*(10) = M \cdot N \cdot k_l \cdot k_s$$

with:

M = reading of the instrument
N = calibration factor
k_l = correction factor for the linearity
k_s = field-specific correction factor.

4. Results

4.1. Calibration factor

The calibration factor for the quantity $\dot{H}^*(10)$ was determined for the following reference conditions: neutron radiation field from the bare ^{252}Cf source with a neutron ambient dose equivalent rate of (71.1 ± 1.8) µSv/h. The result is given in table 2 and is valid for a reading of 186.6 µSv/h for the ^{241} Am-Be(α,n) check source of the PTB.

Tab. 2: Calibration factor

source	calibration factor N
^{252}Cf	1.052 ± 0.029

4.2. Field-specific correction factor

Because of the often undesirable energy-dependent dose-equivalent response of neutron instruments, the uncorrected reading can only be used in radiation fields with the same or similar neutron energy distribution as that of the calibration field. For use in neutron radiation fields with other energy distributions a field-specific correction factor should be applied. For two radiation fields, k_s was determined experimentally (table 3).

Tab. 3: Field-specific correction factor

neutron field	correction factor k_s
^{252}Cf	1
$^{252}Cf(D_2O)$	0.82 ± 0.07
$^{241}Am\text{-}Be(\alpha,n)$	1.04 ± 0.08

For other radiation fields such as work place fields, k_s can be determined by a "field calibration" (i.e. the comparison of the instrument's reading with a reference instrument which can determine the conventional true value in the work place) or by calculation. The latter method requires that the energy dependent fluence response of the instrument and the spectral neutron fluence of the radiation field is known from measurement or calculation /6,7/.

4.3. Correction factor for linearity

The linearity of the reading was tested with four ^{252}Cf-sources of known directional dependence of their neutron source strengths. The correction factors k_l were derived from the ratios of the expected and the observed readings. The correction factors for various instrument readings, normalized to a reading of 90.1 µSv/h, are listed in table 4.

Tab. 4: Correction factors for non-linearity

reading µSv/h	correction factor k_l
529	0.999 ± 0.018
90.1	1
18.0	1.016 ± 0.028
1.9	1.02 ± 0.07

4.4. Photon response of the instrument

According to IEC 61005 /8/ the response of a neutron area monitor to ^{137}Cs gamma radiation with an ambient dose equivalent rate of 10 mSv/h shall not be greater than the response to a neutron ambient dose equivalent rate of 100 µSv/h. In addition, in a field of 1 mSv/h from a neutron reference source, additional exposure to 10 mSv/h from ^{137}Cs gamma radiation shall not change this neutron indication by more than 10 %.

The instrument's response to photon radiation was tested with a ^{137}Cs-source which produced a photon ambient dose equivalent rate of about 10 mSv/h at the reference position. The reading of the integrated dose after 300 s was

$$M_\gamma = 0\ \mu Sv.$$

For testing, whether a reading from a neutron source is influenced by an additional photon source, a reading of

$$M_n = (998 \pm 5)\ \mu Sv/h$$

was produced with a ^{252}Cf-source. An additional exposure by the ^{137}Cs-source (photon ambient dose equivalent rate of about 10 mSv/h) resulted in a reading of

$$M_{n+\gamma} = (1017 \pm 4)\ \mu Sv/h.$$

4.5. Stability check of the instrument reading

During the measurements the stability of the instrument was tested several times with a ^{241}AmBe(α,n)-check source from PTB. At a mean reading of about 186.0 µSv/h the maximum and the minimum values deviated by no more than +1.4 % and –2.2 % from this mean value.

4.6. Background reading

For a measuring time of 3600 s a integral dose of

0.000 μSv

was observed without the presence of neutron sources.

/1/: International Standard ISO 8529-1 *Reference Neutron radiations: Characteristics and methods of production* (2001)
/2/: International Standard ISO 8529-2 *Reference Neutron radiations: Calibration fundamentals of radiation protection devices related to the basic quantities characterizing the radiation field* (2000)
/3/: International Standard ISO 8529-3 *Reference Neutron radiations: Calibration of area and personal dosimeters and determination of their response as a function of neutron energy and angle of incidence* (1998)
/4/: H. Kluge *Irradiation facility with radioactive reference neutron sources: Basic principles* PTB Report, PTB-N-34, 1998
/5/: Jetzke, S. and Kluge, H. *Characteristics of the ^{252}Cf neutron fields in the irradiation facility of the PTB* Radiat. Prot. Dosim., 69, 247 (1997)
/6/: DIN 6802-2 *Neutronendosimetrie: Teil 2: Konversionsfaktoren zur Berechnung der Orts- und Personendosis aus der Neutronenfluenz und Korrektionsfaktoren für Strahlenschutzdosimeter* (1999)
/7/: ICRU 66 *Determination of Operational Dose Equivalent Quantities for Neutrons* (2001)
/8/: IEC 61005 Radiation protection instrumentation – Neutron ambient dose equivalent (rate) meters (2003)

Physikalisch-Technische Bundesanstalt

Die Physikalisch-Technische Bundesanstalt (PTB) in Braunschweig und Berlin ist das nationale Metrologieinstitut und die technische Oberbehörde der Bundesrepublik Deutschland für das Messwesen und Teile der Sicherheitstechnik. Die PTB gehört zum Dienstbereich des Bundesministeriums für Wirtschaft und Technologie. Sie erfüllt die Anforderungen an Kalibrier- und Prüflaboratorien auf der Grundlage der DIN EN ISO/IEC 17025.

Zentrale Aufgabe der PTB ist es, die gesetzlichen Einheiten in Übereinstimmung mit dem Internationalen Einheitensystem (SI) darzustellen, zu bewahren und – insbesondere im Rahmen des gesetzlichen und industriellen Messwesens – weiterzugeben. Die PTB steht damit an oberster Stelle der metrologischen Hierarchie in Deutschland. Kalibrierscheine der PTB dokumentieren die Rückführung des Kalibriergegenstandes auf nationale Normale.

Dieser Ergebnisbericht ist in Übereinstimmung mit den Kalibrier- und Messmöglichkeiten (CMCs), wie sie im Anhang C des gegenseitigen Abkommens (MRA) des Internationalen Komitees für Maße und Gewichte enthalten sind. Im Rahmen des MRA wird die Gültigkeit der Ergebnisberichte von allen teilnehmenden Instituten für die im Anhang C spezifizierten Messgrößen, Messbereiche und Messunsicherheiten gegenseitig anerkannt (nähere Informationen unter http://www.bipm.org).

CIPM MRA

The Physikalisch-Technische Bundesanstalt *(PTB) in Braunschweig and Berlin is the National Metrology Institute and the highest technical authority of the Federal Republic of Germany for the field of metrology and certain sectors of safety engineering. The PTB comes under the auspices of the Federal Ministry of Economics and Technology. It meets the requirements for calibration and testing laboratories as defined in the EN ISO/IEC 17025.*

It is fundamental task of the PTB to realize and maintain the legal units in compliance with the International System of Units (SI) and to disseminate them, above all within the framework of legal and industrial metrology. The PTB thus is on top of the metrological hierarchy in Germany. Calibration certificates issued by it document that the object calibrated is traceable to national standards.

This certificate is consistent with Calibration and Measurement Capabilities (CMCs) that are included in Appendix C of the Mutual Recognition Arrangement (MRA) drawn up by the International Committee for Weights and Measures (CIPM). Under the MRA, all participating institutes recognize the validity of each other's calibration and measurement certificates for the quantities, ranges and measurements uncertainties specified in Appendix C (for details see http://www.bipm.org).

Physikalisch-Technische Bundesanstalt
Bundesallee 100
38116 Braunschweig
DEUTSCHLAND

Abbestraße 2-12
10587 Berlin
DEUTSCHLAND

List of Tables

List of Equations

List of Figures

References

[1] International Standard ISO 8529, Neutron Reference Radiation for Calibrating Neutron-Measuring Devices used for Radiation Protection Responses and for Determining their Response as a Function of Neutron Energy; ISO 8529:1989 (E).

[2] International Standard ISO 8529-3, Reference Neutron Radiations – Part 3: Calibration of Area and Personal Dosimeters and Determination of their Response as a Function of Neutron Energy and Angle of Incidence; ISO 8529-3:1998 (E).

[3] International Standard ISO 10647, Procedure for Calibrating and Determining the Response of Neutron-Measuring Devices used for Radiation Protection Purposes; ISO 10647:1996 (E).

[4] Burger, G., Schwartz, R. B., 1988. Guidelines on Calibration of Neutron Measuring Devices, IAEA Technical Report Series No. 285. International Atomic Energy Agency, Vienna.

[5] Chabot, G. E., et al., 1991. Calibration of Survey Instruments Used in Radiation Protection for the Assessment of Ionizing Radiation Fields and Radioactive Surface Contamination; NCRP Report No. 112, National Council on Radiation Protection and Measurements, USA.

[6] Hunt, J. B., 1984. The Calibration of Neutron Sensitive Spherical Devices, Radiation Protection Dosimetry 8(4), 239-251.

[7] Eisenhauer, C., M., et al., 1982. Measurement of Neutrons Reflected from the Surfaces of a Calibration Room, Health Physics 42(4), 489-495.

[8] Eisenhauer, C., M., 1989. Review of Scattering Corrections for Calibration of Neutron Instruments; Radiation Protection Dosimetry 28(4), 253-262.

[9] Eisenhauer, C., M., 1985. Calibration Techniques for Neutron Personal Dosimetry, Radiation Protection Dosimetry 10(1-4), 43-57.

[10] Cruz, M. T., Fratin, L., 1992. Establishment of a Procedure for Calibrating Neutron Monitors at the Physics Institute of the University of Sao Paulo, Brazil, Radiation Protection Dosimetry 44(1-4), 143-146.

[11] Hunt, J. B., 1976. The Calibration and Use of Long Counters for the Accurate Measurement of Neutron Flux Density; NPL Report RS(EXT)5, ISSN 0143-7135.

[12] Pipes, L. A., Harvill, L. R., 1971. Applied Mathematics for Engineering and Physicists, 3rd Ed., McGraw-Hill International Book Company, 8th printing 1982.

[13] Stroud, K. A., 1982. Engineering Mathematics, Programs & Problems; 2nd Ed., MacMillan Press LTD.

[14] Southworth, R. W., Deleeuw S. L., 1965. Digital Computation and Numerical Methods. McGraw-Hill Book Company.

[15] Guide to The Expression of Uncertainty in Measurements (GUM). 1993, 1st Ed., BIPM, IEC, IFCC, ISO, IUPAC, IUPAP and OIML, ISBN 92-67-10188-9.

[16] Caria, M., 2000. Measurement Analysis 'An Introduction to the Statistical Analysis of Laboratory Data in Physics, Chemistry and the Life Sciences'. Imperial College Press.

[17] Lira, I., 2002. Evaluating the Measurement Uncertainty 'Fundamental and Practical Guidance', Series in Measurement Science and Technology, Institute of Physics Publishing, Bristol & Philadelphia.

[18] Periodical Table, Sergent-Welch Scientific Company, Illinois, USA.

[19] Neutron Scattering Length and Cross Section, NIST Center for Neutron Research, USA, Online: http://www.ncnr.nist.gov/resources/n-lengths/list.html, accessed in June 2009.

[20] Certificate of Measurement of ^{241}Am/Be neutron source, serial No. 4232NE, 1982. NPL Reference N113.

[21] Drawing Reference AOE 116313, ANSTO Engineering, 2006.

[22] Wolfram, S., 2003. Mathematical Computing System package, Version 5.

[23] Curtiss, L. F., 1959. Introduction to Neutron Physics, D. Van Nostrand Company Inc.

[24] Wikipedia online: http://en.wikipedia.org/wiki/paraffin_wax, accessed in June 2009.

[25] Neutron Monitor Model 2222, Wedholm Medical. Online: http://www.wedholmmedical.se, accessed in June 2009.

ANSTO Report No. E-773

ISBN 1 921268 123